

# The Multivariate Bernoulli detector: Change point estimation in discrete survival analysis

Willem van den Boom<sup>1,\*</sup>, Maria De Iorio<sup>1,2,\*\*</sup>, Fang Qian<sup>1,\*\*\*</sup>, and Alessandra Guglielmi<sup>3,\*\*\*\*</sup>

<sup>1</sup>Yong Loo Lin School of Medicine, National University of Singapore

<sup>2</sup>Singapore Institute for Clinical Sciences, Agency for Science, Technology and Research

<sup>3</sup>Department of Mathematics, Politecnico di Milano, Milan, Italy

\**email*: vandenboom@nus.edu.sg

\*\**email*: mdi@nus.edu.sg

\*\*\**email*: qianxiaoxie@gmail.com

\*\*\*\**email*: alessandra.guglielmi@polimi.it

**SUMMARY:** Time-to-event data are often recorded on a discrete scale with multiple, competing risks as potential causes for the event. In this context, application of continuous survival analysis methods with a single risk suffer from biased estimation. Therefore, we propose the Multivariate Bernoulli detector for competing risks with discrete times involving a multivariate change point model on the cause-specific baseline hazards. Through the prior on the number of change points and their location, we impose dependence between change points across risks, as well as allowing for data-driven learning of their number. Then, conditionally on these change points, a Multivariate Bernoulli prior is used to infer which risks are involved. Focus of posterior inference is cause-specific hazard rates and dependence across risks. Such dependence is often present due to subject-specific changes across time that affect all risks. Full posterior inference is performed through a tailored local-global Markov chain Monte Carlo (MCMC) algorithm, which exploits a data augmentation trick and MCMC updates from non-conjugate Bayesian nonparametric methods. We illustrate our model in simulations and on ICU data, comparing its performance with existing approaches.

**KEY WORDS:** Bayesian statistics; competing risks; discrete failure time models; discrete time-to-event data; grouped survival data; local-global Markov chain Monte Carlo.

## 1. Introduction

Time-to-event data are common in many applications such as finance, medicine and engineering with examples including time to payment, and survival and failure times. Most approaches to survival data consider continuous event times. Nevertheless, it is more and more common to record time-to-event data on a discrete scale (e.g. patient-reported outcomes, or time to pregnancy measured in number of menstrual cycles it takes a couple to conceive). See [Schmid and Berger \(2020\)](#) for further examples. Discrete recording of the timings of events ([Allison, 1982](#)) may occur when time is truly discrete, or when continuous time is partitioned into non-overlapping intervals (corresponding, for instance, to days, weeks, or months) and only the interval in which an event occurs is recorded ([King and Weiss, 2021](#)). This special case of interval censoring is usually referred to as *grouped time* and, in this work, we consider discrete survival models that arise as probabilistic grouped versions of continuous-time frailty models from survival analysis (see, e.g., [Hougaard, 1986, 1995](#); [Andersen et al., 1993](#), Chapter IX; [Hougaard, Myglegaard, and Borch-Johnsen, 1994](#); [Kalbfleisch and Prentice, 2002](#)). Indeed, direct application of continuous-time methods to discretely recorded data may result in biased estimation ([Lee et al., 2018](#)).

Moreover, our focus is on discrete survival data in the presence of multiple, competing risks that can cause an event. Traditional analyses often consider a single risk with events due to other risks, e.g. other causes of death, treated as censoring. However, this generally violates the common assumption of independent censoring ([Schmid and Berger, 2020](#)). Moreover, such analyses can lead to misestimation of hazards and covariate effects ([Andersen et al., 2012](#)). Here we consider data from the Medical Information Mart for Intensive Care IV (MIMIC-IV, [Johnson et al., 2023](#)) database on length of stay in an intensive care unit (ICU), typically reported discretely in days. While the MIMIC-IV database documents admission and discharge times down to the minute, it is recommended to perform survival analysis using

discrete day units. This approach is preferred because admission and discharge times within a single day are significantly determined by hospital protocols and staff decisions, rather than purely reflecting the patients' health conditions. The study considers three competing events that can terminate an ICU stay: discharge to home (69.0%), transfer to another medical facility (21.4%), and in-hospital death (6.1%).

The two main approaches for competing risks with discrete times are cause-specific hazard functions and the subdistribution hazard model ([Schmid and Berger, 2020](#)). The latter is more suitable when interest is in one out of many risks. The first approach usually exploits methods from generalized linear models (GLMs), enabling maximum likelihood estimation, variable selection and other methods from GLMs such as in [Tutz \(1995\)](#) and [Möst, Pöbnecker, and Tutz \(2016\)](#). Our work places itself within this approach, focussing on scenarios with few risks and thus considers cause-specific hazards, i.e. a hazard function for each risk, introducing dependence across risks by building on recent advances in change point analysis.

A characteristic of traditional discrete survival models as compared to GLMs is that they present unconstrained baseline hazards. This leads to a large number of parameters to estimate and, as a consequence, to unstable estimation, especially if for certain time points the number of events is small. To improve stability, regularizations of hazard functions have been proposed. See, for example, [Luo, Kong, and Nie \(2016\)](#), [Heyard et al. \(2019\)](#) and [Möst et al. \(2016\)](#). [Fahrmeir and Wagenpfeil \(1996\)](#) and [King and Weiss \(2021\)](#) employ random walks to smooth the hazard function. In all these works, cause-specific baseline hazards are treated independently. [Vallejos and Steel \(2017\)](#) focus on risk-specific covariate selection, still assuming independence across risks. On the other hand, dependence across risks is plausible since multiple hazards can be affected by changes to the individual across time, and as such should be incorporated in the model.

The main methodological contribution of this work lies in modeling explicit and inter-

pretable dependencies across risks. We introduce a multivariate change point model for baseline hazards, which offers two key advantages (Kozumi, 2000). Firstly, it reduces the number of parameters, promoting parsimony. Secondly, it accommodates the variability in hazard rates across different survival times. We adopt a Bayesian approach, assigning priors on the number and location of overall change points, inducing marginal dependence among them. For each overall change point, we use a Multivariate Bernoulli prior to determine which risks are involved, a method previously applied in time series analysis (Dobigeon, Tourneret, and Davy, 2007; Harlé et al., 2016). We term our approach the Multivariate Bernoulli detector, building on prior work by Harlé et al. (2016).

Change points have been widely studied in continuous survival analysis (e.g. Matthews and Farewell, 1982; Goodman, Li, and Tiwari, 2011) but less so in the discrete case: Kozumi (2000) considers a single risk modeled via a Markov chain with a prespecified number of change points, while Wang and Ghosh (2007) use posterior predictive checks for change point detection, without allowing for covariates in the model. On the other hand, we allow for covariates in the model and perform cause-specific variable selection. Moreover, we estimate the number of change points, testing for the presence and location of change points using Bayes factors or posterior probabilities.

The paper is structured as follows. Section 2 introduces the model and describes a tailored Markov chain Monte Carlo (MCMC) sampler. Section 3 discusses an application to the ICU data. Section 4 compares our approach with existing ones. We conclude the paper in Section 5.

## 2. Model

### 2.1 Setup and notation

We follow the notation in [Tutz and Schmid \(2016\)](#). Let  $T_i$  denote the time to event for individual  $i \in \{1, \dots, n\}$  where  $n$  is the number of individuals. In the discrete-time setting,  $T_i \in \{1, \dots, t_{\max} + 1\}$  for some maximum time  $t_{\max}$ . The random variable  $T_i$  can for instance arise as the discretization, also known as grouping ([Kalbfleisch and Prentice, 2002](#)), of a latent continuous time  $T_i^c$  into  $t_{\max} + 1$  intervals  $[\omega_0, \omega_1)$ ,  $[\omega_1, \omega_2)$ ,  $\dots$ ,  $[\omega_{t_{\max}}, \infty)$  with  $\omega_0 = 0$ . In this case there is a one-to-one correspondence between the set of integers  $\{1, \dots, t_{\max} + 1\}$  and the intervals of the real line where the continuous-time random variables  $T_i^c$  are defined. As such, the interpretation of  $T_i = t_{\max} + 1$  is similar to censoring, in the sense that the event will occur at time  $t > t_{\max}$  (i.e.  $T_i^c \geq \omega_{t_{\max}}$ ) and  $t_{\max} + 1$  is simply a “latent time” that groups together individuals for which it is known that the event has not occurred up to time  $t_{\max}$ . The time-to-event distribution is usually characterized by the overall hazard function  $\lambda(t | \theta_i) = P(T_i = t | T_i \geq t, \theta_i) = P\{T_i^c \in [\omega_{t-1}, \omega_t) | T_i^c \geq \omega_{t-1}, \theta_i\}$  for some vector of parameters  $\theta_i$ .

Additionally, we assume that observations are subject to censoring. That means that only a portion of the observed times can be considered as exact survival times. Let  $C_i$  be the censoring time of individual  $i$ .  $C_i$  assumes values in  $\{1, \dots, t_{\max}\}$ , with  $T_i$  and  $C_i$  independent (random censoring). Moreover, we assume that the censoring mechanism is non-informative, i.e. it does not depend on any parameters used to model the event times ([Schmid and Berger, 2020](#)). Let  $\delta_i = \mathbb{1}[T_i \leq C_i]$  be a censoring indicator, where  $\mathbb{1}[\cdot]$  denotes the indicator function, and  $t_i = \min(T_i, C_i)$  the observed time.

We consider competing risks with  $m$  different types of events. For instance, the events can correspond to death due to  $m$  different causes. Then,  $R_i \in \{1, \dots, m\}$  denotes the event type experienced by individual  $i$  at time  $T_i$ , for which we observe a value  $r_i$  only in the

absence of censoring, i.e.  $\delta_i = 1$ . Finally, the cause-specific hazard function is  $\lambda_r(t | \theta_i) = P(T_i = t, R_i = r | T_i \geq t, \theta_i)$  such that  $\lambda(t | \theta_i) = \sum_{r=1}^m \lambda_r(t | \theta_i)$ .

## 2.2 Likelihood

We assume independence across individuals such that the likelihood is a product over individual-specific terms. For ease of explanation, we consider the likelihood contribution of one individual and drop subscripts  $i$  in the remainder of this section unless otherwise specified. Under the assumption that  $C$  is independent of  $T$  and  $\theta$ , the likelihood for  $\theta$  is given by

$$P(T = t, R = r | \theta)^\delta P(T > t | \theta)^{1-\delta} = \lambda_r(t | \theta)^\delta \prod_{l=1}^{t-\delta} \{1 - \lambda(l | \theta)\} \quad (1)$$

and we specify  $\lambda_r(t | \theta)$  and thus  $\lambda(t | \theta)$  according to the multinomial logit model which is the most popular for categorical responses (Tutz and Schmid, 2016). Specifically,  $\lambda_r(t | \theta) = \exp(\eta_{rt}) / \{1 + \sum_{\rho=1}^m \exp(\eta_{\rho t})\}$  where  $\eta_{rt} = \alpha_{rt} + \mathbf{x}^\top \boldsymbol{\beta}_r$  is a cause- and time-specific linear predictor, and  $\theta = \{\eta_{rt}\}$ . The intercept  $\alpha_{rt}$  represents the cause-specific baseline hazard. The  $p$ -dimensional vector  $\boldsymbol{\beta}_r = (\beta_{r1}, \dots, \beta_{rp})$  consists of the cause-specific regression coefficients of the covariates in the  $p$ -dimensional vector  $\mathbf{x} = (x_1, \dots, x_p)$ . Such likelihood specification is also known as proportional continuation ratio model (Tutz and Schmid, 2016) as increasing  $x_j$  by one unit increases the cause-specific odds by the factor  $\exp(\beta_{rj})$ . Note that, when  $r = 1$  and  $\delta = 1$ ,  $\lambda_r(t | \theta)$  corresponds to  $\phi_t$  defined in Section 2.5 and the considerations on prior specification there discussed will be relevant when building a change point model on  $\alpha_{rt}$ .

## 2.3 The Multivariate Bernoulli detector

We propose a model on the baseline hazards that is flexible, yet has interpretable structure. Specifically, the sequence  $\alpha_{r1}, \dots, \alpha_{r,t_{\max}}$  is set to follow a piecewise constant function. We do so through a change point model with dependence across risks  $r$ . In our setup, a change point corresponds to a time point where the hazard of at least one risk  $r$  changes. We specify

a hierarchical prior on the change points which has three main components: (i) a prior on the number of change points; (ii) a prior on the location of change points; (iii) and a prior on which risks (at least one) have a change point at that particular time location, given that a change point at time  $t$  occurs.

*2.3.1 Prior specification on overall change points.* In this section, we describe prior specification on the number and location of change points. Let  $\boldsymbol{\alpha}_t = (\alpha_{1t}, \dots, \alpha_{mt})$ . Then,  $\gamma_t = \mathbb{1}[\boldsymbol{\alpha}_t \neq \boldsymbol{\alpha}_{t-1}]$  indicates whether there is an overall change point at  $t \in \{1, \dots, t_{\max}\}$ , i.e. if the hazard of at least a risk changes at time  $t$ . Furthermore,  $K = \sum_{t \in \mathcal{T}} \gamma_t$  denotes the number of change points. Here  $\mathcal{T}$  defines the set of possible change point locations. We specify the prior on  $\boldsymbol{\gamma} = (\gamma_1, \dots, \gamma_{t_{\max}})$  hierarchically, by specifying a prior  $p(K)$  on the number of change points and then  $p(\boldsymbol{\gamma} | K)$  as this provides explicit regularization on  $K$ : i.i.d.  $\gamma_t$  would imply a binomial distribution on  $K$ .

To motivate the next model development, consider the bottom plots in Figure 2 where two observations with  $t_i = 7$  out of 500 are not used when inferring change points. Then, the lack of observations at time  $t = 7$  results in spurious change points at that time location and the next. We restrict our inference to avoid such sensitivity to a few observations: to aid identifiability, considering the flexibility of the underlying Time-Varying Geometric distribution which is discussed in Section 2.5, we only allow change points for a subset of times  $\mathcal{T} \subset \{1, \dots, t_{\max}\}$  such that  $\gamma_t = 0$  if  $t \notin \mathcal{T}$ . Firstly, as it is typical in change point applications, we do not allow change points at the support boundary, in our case  $t = 1$  and  $t = t_{\max}$ . Moreover, we do not allow a change point at time  $t$  if both  $t$  and  $t - 1$  have no observed events as the data lack information on which of the two time points would be a change point. Also, we do not allow change points at a time  $t$  with no observed events if both neighboring times  $t - 1$  and  $t + 1$  have observed events, because this would lead to spurious change points due to the flexibility of the underlying Time-Varying Geometric,

as seen in Figure 2 (bottom row). On the other hand, we prefer to introduce parsimony in the estimation of change points to improve interpretability. We explore the effect of the restriction on change point locations in a simulation study in Web Section E.4. There, the restriction (i) does not deteriorate inference, even if the true change point is not in  $\mathcal{T}$ ; (ii) avoids spurious change points at time locations without observed events.

We assume a Geometric distribution with success probability  $\pi_K$  truncated to  $K \leq |\mathcal{T}|$  as prior on the number of change points. We denote such prior as  $\text{Geo}_{|\mathcal{T}|}(\pi_K)$ . For the locations of overall change points given  $K$ , we use the uniform distribution on possible configurations  $p(\boldsymbol{\gamma} | K) = 1/\binom{|\mathcal{T}|}{K}$ . In summary, the joint prior on the number and location of change points has a hierarchical specification:  $p(K, \boldsymbol{\gamma}) = p(K) p(\boldsymbol{\gamma} | K)$ .

**2.3.2 Cause-specific change point configuration.** In this section, we discuss the prior on which risks present a jump in the hazard, given the vector  $\boldsymbol{\gamma}$ . Let  $z_{rt} = \mathbb{1}[\alpha_{rt} \neq \alpha_{r(t-1)}]$  be an indicator variable denoting if a change point occurs at time  $t$  for risk  $r$ . If there is no change point at  $t$  for any  $r$ , then  $\gamma_t = 0$  and  $z_{rt} = 0$ . If  $\gamma_t = 1$ , then  $z_{rt} = 1$  for at least one  $r$ .

Let  $\mathbf{z}_t = (z_{1t}, \dots, z_{mt})$ . Conditionally on  $\gamma_t = 1$ , we assume that  $\mathbf{z}_t$  follows a Multivariate Bernoulli distribution (e.g. Teugels, 1990). An  $m$ -dimensional binary vector  $\mathbf{z}_t$  can assume  $2^m$  possible values corresponding to a combination of  $z_{rt} \in \{0, 1\}$ . The Multivariate Bernoulli distribution is then parameterized by a  $2^m$ -dimensional vector, whose elements correspond to the probability of each particular outcome (i.e. configuration). In our case, when modeling  $\mathbf{z}_t$  given  $\gamma_t = 1$ , we exclude the configuration of all zeros, i.e.  $z_{rt} = 0$  for every  $r$ . Thus,  $\mathbf{z}_t$  can assume only  $2^m - 1$  possible values. We denote such distribution as  $\text{Ber}_0(\boldsymbol{\psi})$ , where  $\boldsymbol{\psi}$  denotes the  $(2^m - 1)$ -dimensional vector of configuration probabilities. In summary, the prior specification for  $\mathbf{z}_t$  is

$$\mathbf{z}_t | \gamma_t \sim \begin{cases} \text{Ber}_0(\boldsymbol{\psi}) & \text{if } \gamma_t = 1 \\ \delta_{\mathbf{0}} & \text{if } \gamma_t = 0 \end{cases}$$



where  $\delta_{\mathbf{0}}$  is a point mass at the zero vector. We refer to the joint prior on  $(K, \boldsymbol{\gamma}, \mathbf{z})$  as Multivariate Bernoulli detector, where  $\mathbf{z} = \{\mathbf{z}_t\}_{t=1}^{t_{\max}}$ .

#### 2.4 Further prior specification

Model specification is completed by specifying independent prior distributions on  $\alpha_{rt}$  and  $\boldsymbol{\beta}_r$ . We specify a prior on  $\alpha_{rt}$  conditionally on the number and location of change points. Since  $\boldsymbol{\alpha}_r = (\alpha_{r1}, \dots, \alpha_{rt_{\max}})$  is a piecewise constant function for each risk  $r$ , assuming constant values between change points, let  $\alpha_{r\ell}^*$  denote the unique value of  $\alpha_{rt}$  over each time interval for risk  $r$ . Note that for each risk a change point can be activated or not, with the only constraint that a change point needs to be activated for at least one risk. We assume  $\alpha_{r\ell}^* \sim \mathcal{N}(\mu_\alpha, \sigma_\alpha^2)$  independently across  $\ell$  and  $r$ .

Furthermore, to identify important effects, we assume a variable selection prior for the regression coefficients,  $\boldsymbol{\beta}_r = (\beta_{r1}, \dots, \beta_{rp})$ , which allows for risk-specific variable selection. Here, we consider a spike-and-slab prior (Mitchell and Beauchamp, 1988):  $\beta_{rj} \sim \pi_\beta \mathcal{N}(0, \sigma_\beta^2) + (1 - \pi_\beta) \delta_0$  where  $\pi_\beta$  is the prior inclusion probability. We use the hyperprior  $\pi_\beta \sim \mathcal{U}(0, 1)$ . In the application in Section 3, some variables are grouped as they are dummy variables associated with a categorical covariate. We modify the prior accordingly to perform groupwise variable selection as detailed in Web Appendix B. We note that other possible prior choices are available in the literature to perform variable selection, such as shrinkage priors (Bhadra et al., 2019), which offer computational advantages, at the cost of depending on arbitrary thresholds to identify relevant effects.

In the simulation studies and the application on ICU data, we set the parameters as follows:  $\sigma_\beta^2 = 1$ ,  $\pi_K = 0.5$ , all elements of  $\boldsymbol{\psi}$  equal to  $1/(2^m - 1)$ ,  $\mu_\alpha = -9$  and  $\sigma_\alpha^2 = 3$ . The particular prior choice for  $\alpha_{r\ell}^*$  derives from the interpretation of the model in terms of the Time-Varying Geometric. In Section 2.5, we highlight the importance of shrinking the probabilities  $\phi_t$  towards zero. This is equivalent, in absence of covariates, to shrinking

$\exp(\alpha_{r\ell}^*)/\{1 + \exp(\alpha_{r\ell}^*)\}$  towards zero and, consequently,  $\alpha_{r\ell}^*$  towards  $-9$ . Roughly speaking, a  $\mathcal{N}(-9, 3)$  on  $\alpha_{r\ell}^*$  is equivalent to a  $\text{Beta}(0.01, 1)$  prior on  $\phi_t$ , which is shown to have a good performance in Section 2.5. Finally, we note that we could specify a prior on  $\boldsymbol{\psi}$  to favor sparsity or a large number of change points.

### 2.5 Rationale behind modeling strategy

Prior specification for the parameters governing the Multivariate Bernoulli detector (see Section 2.4) is derived from the following considerations. In the uncensored ( $\delta = 1$ ) single-risk ( $m = 1$ ) case, the distribution of the time to event in the discrete case is a Time-Varying Geometric distribution (Landau and Zachmann, 2019) with time-varying success probability  $\phi_t = \lambda(t \mid \theta)$ , i.e.

$$P(T = t \mid \{\phi_l\}_l) = \begin{cases} \phi_t \prod_{l=1}^{t-1} (1 - \phi_l), & t = 1, \dots, t_{\max} \\ \prod_{l=1}^{t-1} (1 - \phi_l), & t = t_{\max} + 1 \end{cases} \quad (2)$$

The Time-Varying Geometric is fully flexible in that it can represent any distribution on  $\{1, \dots, t_{\max} + 1\}$  by appropriately choosing  $\phi_t$  (Mandelbaum, Hlynka, and Brill, 2007). It is analogous to the Piecewise Exponential distribution in continuous survival analysis (Gamerman, 1991), if we assume a change point model for the  $\phi_t$ . See Figure 1 for widely varying realisations of the distribution for certain  $\{\phi_t\}_t$ . This flexibility should be taken into account when inferring  $\phi_t$ . It relates to the potential lack of stability of unconstrained estimation of baseline hazards mentioned in Section 1. For instance, there is a separate parameter  $\phi_t$  for each time point, but we might not have observed an event at each time point. To avoid such overparameterization, some subsequent  $\phi_t$  can be assumed to be equal to each other, as in Figure 1, resulting in a change point model: a change point is a time  $t$  for which  $\phi_t \neq \phi_{t-1}$ . Moreover, given the flexibility of the Time-Varying Geometric, different combinations of  $\{\phi_t\}$  can lead to a satisfactory fit of a data set, leading to identifiability

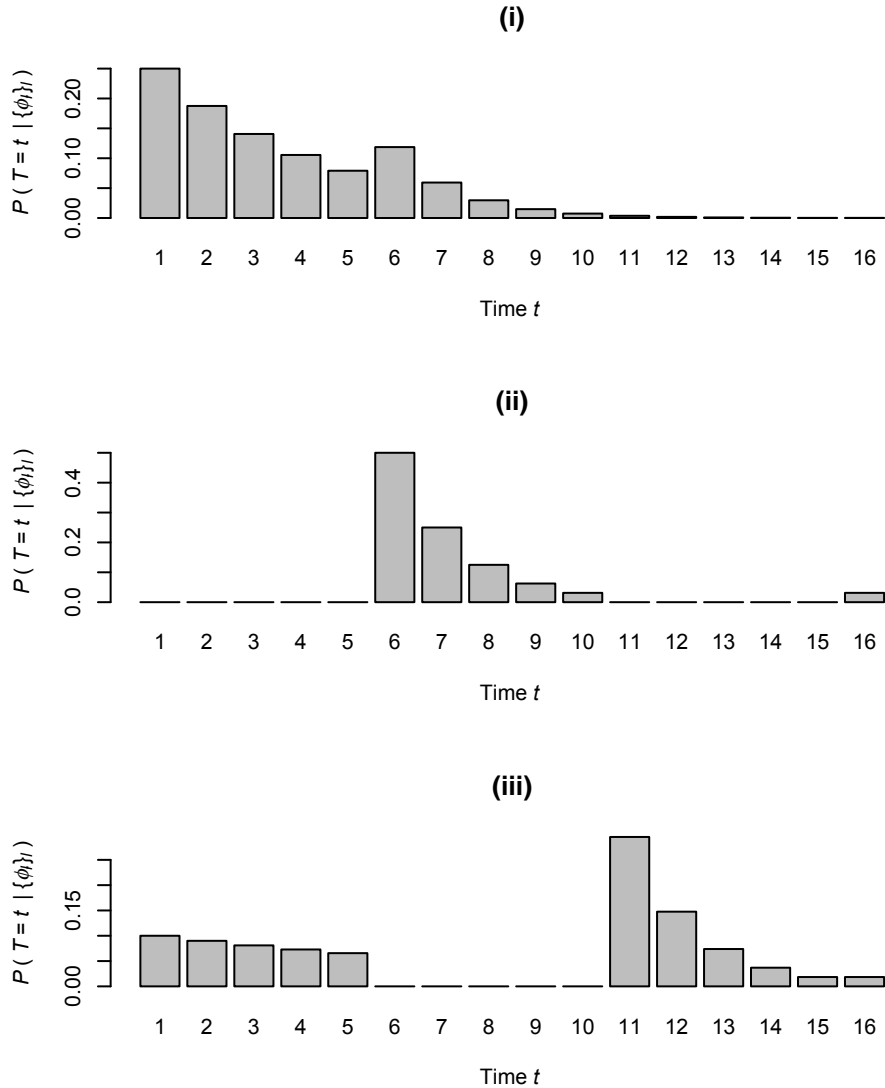


**Figure 1.** Probability mass function of the Time-Varying Geometric distribution: Visualizations of (2) with  $t_{\max} = 15$  and success probabilities (i)  $\phi_t = 0.25$  for  $t \leq 5$  and  $\phi_t = 0.5$  otherwise; (ii)  $\phi_t = 0$  for  $t \leq 5$  or  $t \geq 11$ , and  $\phi_t = 0.5$  otherwise; (iii)  $\phi_t = 0.1$  for  $t \leq 5$ ,  $\phi_t = 0.5$  for  $t \geq 11$  and  $\phi_t = 0$  otherwise.

problems. As such, we impose prior regularization by a priori shrinking the value of  $\phi_t$  towards zero. We further motivate our prior choice in the following simulation study.

We simulate  $n = 500$  times  $t_i$  from (2) with  $t_{\max} = 1000$  using two different settings for  $\phi_t$ . We consider a scenario without change points with  $\phi_t = 0.5$ , and a scenario with a single

change point given by  $\phi_t = 0.5$  for  $t \leq 4$  and  $\phi_t = 0.25$  for  $t \geq 5$ . For this last scenario, we also consider the data after removal of observations with  $t_i = 7$ , which we discuss in Section 2.3.1 in relation to the prior constraints on change point location. To understand how the prior on  $\phi_t$  can affect inference on change points, we compare two priors within a Bayesian change point model defined as follows: we specify a uniform prior over all possible change point configurations among the  $\phi_t$ . Let  $\phi_\ell^*$  denote the unique value of  $\phi_t$  over each time interval delimited by the change points. Conditionally on a change point configuration, we choose a prior on  $\phi_\ell^*$ . Then, the likelihood in (2) completes the model. We fit this model with  $t_{\max} = \max_i t_i$ , such that  $t_{\max} = 9$  for the data with no change point and  $t_{\max} = 14$  for the data with a change point. We compare posterior inference obtained with a uniform prior,  $\phi_\ell^* \sim \mathcal{U}(0, 1)$ , and with a prior that shrinks the parameters towards zero,  $\phi_\ell^* \sim \text{Beta}(0.01, 1)$ .

Figure 2 shows the inference on change points. The uniform prior (left column) leads to the detection of too many change points, especially at larger  $t$ . Regularization towards zero using  $\phi_\ell^* \sim \text{Beta}(0.01, 1)$  (right column) yields more accurate posterior inference without spurious change points.

## 2.6 Posterior computation using local-global MCMC

To devise an MCMC scheme to perform posterior inference, we exploit the representation of the likelihood in (1) as a multinomial logistic regression (Tutz and Schmid, 2016), using a data augmentation trick. This results in the availability of conjugate updates, leading to more efficient mixing and preventing, at the same time, large changes in the configuration of change points, resulting in more effective local moves. The latent variables associated with the data augmentation are highly correlated with the change points, and, as such, it is difficult to explore the change points space conditionally on the latent variables. To counterbalance this drawback, we also devise global moves of change points conditionally on the observed data. Such moves are based on ideas from the Bayesian nonparametric literature (Dahl, 2005;

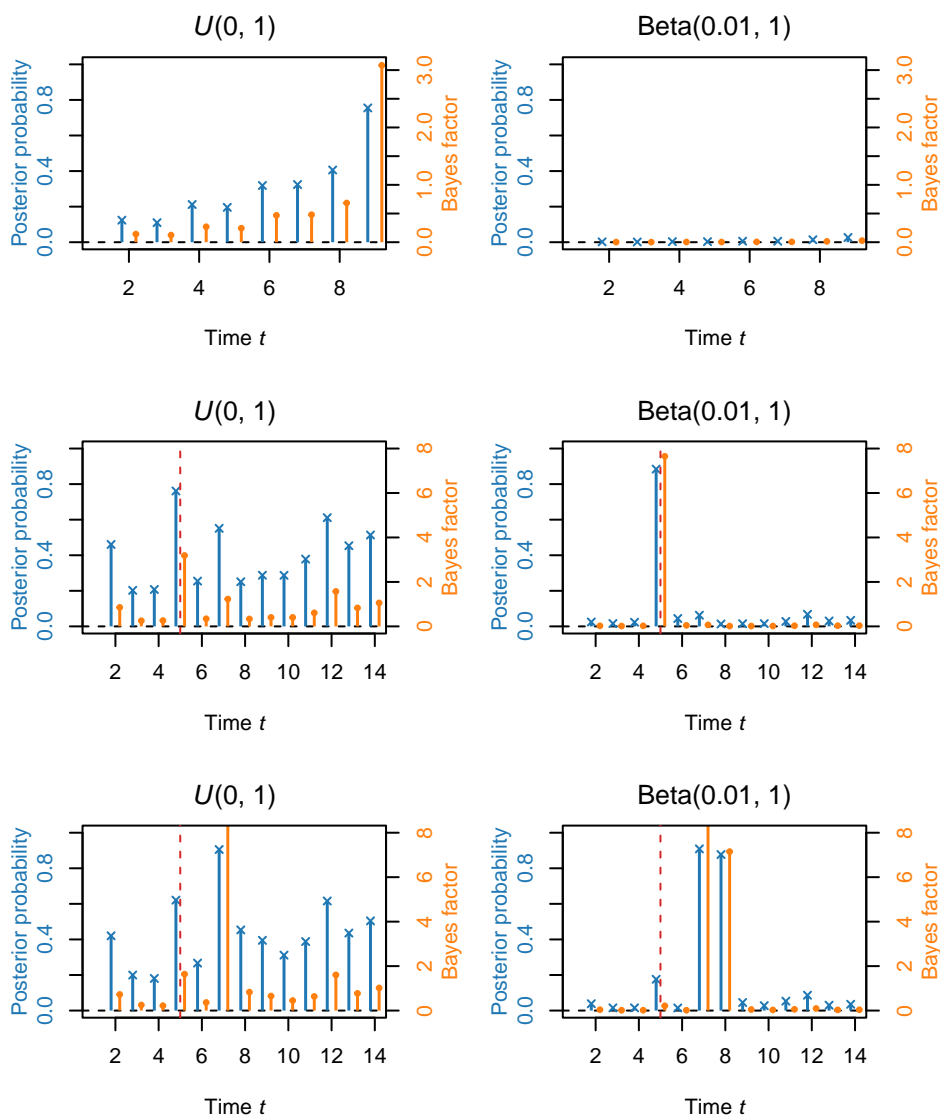


**Figure 2.** Time-Varying Geometric simulation: Posterior probabilities ( $\times$ ) and Bayes factors ( $\bullet$ ) for the presence of a change point with a uniform prior (left column,  $\phi_\ell^* \sim \mathcal{U}(0, 1)$ ) and regularization towards zero (right column,  $\phi_\ell^* \sim \text{Beta}(0.01, 1)$ ) when simulating data without (top row) and with (middle and bottom rows) a change point. The bottom row uses the data from the middle row without the observations with  $t_i = 7$ . The orange lines correspond to Bayes factors, some of which are outside the plotting range. The dashed red lines are drawn in correspondence of the true change point.

Martínez and Mena, 2014; Creswell et al., 2020). Finally, from the MCMC output, we can derive Bayes factors to test for the presence of change points, using the Savage-Dickey ratio (Dickey, 1971; Verdinelli and Wasserman, 1995) (see Web Appendix C for details).

We refer to the resulting hybrid algorithm as “local-global MCMC” borrowing the terminology from Samsonov et al. (2022). Here, we provide a brief explanation of our MCMC strategy in relation to previous work. Web Appendix D details the algorithm.

*2.6.1 Local MCMC with data augmentation.* We exploit the data augmentation representation of a multinomial logistic regression in terms of Gumbel latent variables by McFadden (1974) and Frühwirth-Schnatter and Frühwirth (2007). Then, the augmented likelihood is Gaussian which enables convenient MCMC updates. Importantly, conditionally on the  $z_{rt}$ , the  $\alpha_{r\ell}^*$  have a Gaussian prior such that they can be integrated out from the augmented posterior, enabling efficient updates of  $z_{rt}$  and  $\gamma_t$  without having to specify Metropolis-Hastings proposals for  $\alpha_{r\ell}^*$ .

More recently, other augmentations have been proposed in the literature (see, for instance, Held and Holmes, 2006; Frühwirth-Schnatter and Frühwirth, 2010; Polson, Scott, and Windle, 2013; Linderman, Johnson, and Adams, 2015). We do not opt for them because they do not provide a convenient augmented likelihood in the presence of multiple risks.

*2.6.2 Global MCMC.* Augmented data can strongly reflect the change points of the current state of the MCMC chain, resulting in local MCMC updates to the change point parameters  $z_{rt}$  and  $\gamma_t$ . Therefore, we also consider MCMC moves without data augmentation, i.e. based on the original data, to enable more global change point updates and explore better posterior space.

Specifically, we exploit the fact that change points induce a partition of time into intervals and apply ideas from Bayesian nonparametrics (Dahl, 2005; Martínez and Mena, 2014; Creswell et al., 2020) to deal with non-conjugate updates. This allows for more global moves

at the cost of having to specify Metropolis-Hastings proposals for  $\alpha_{r\ell}^*$ . Alternating between local and global MCMC steps allows for better mixing and convergence of the algorithm.

We demonstrate the performance of our approach in simulation studies. Web Appendix E presents simulation studies with a wide range of scenarios and comparison with alternative models. We find that the Multivariate Bernoulli detector generally results in the most accurate estimation. Prior shrinkage of baseline hazards can result in estimation bias, which is a common feature of Bayesian shrinkage priors and the bias-variance trade-off they induce (e.g. Polson and Sokolov, 2019).

### 3. Application to ICU length of stay

#### 3.1 Data description and analysis

We apply our model to data on ICU stays from the MIMIC-IV database (Johnson et al., 2023) with length of stay as outcome (Meir and Gorfine, 2023).

See Web Appendix A for a detailed data description. We consider  $m = 3$  competing risks: discharge to home, transfer to another medical facility and in-hospital mortality. Length of stay is recorded in days with the longest uncensored time being 28 days. We analyse  $n = 25159$  ICU stays with 17357 discharged to home, 5379 transferred, 1529 deaths and 894 censored. We include the following covariates: demographics, variables related to the ICU stay (e.g. whether it is a repeat admission) and lab tests from the first day. Most covariates are categorical with two or more levels. Representing them as dummy variables leads to a total of  $p = 36$  predictors.

We fit our model with  $t_{\max} = \max_i t_i = 28$  days using 200000 MCMC iterations, discarding the first 50000 as burn-in. The trace plots in Web Figure 14 suggest satisfactory convergence.

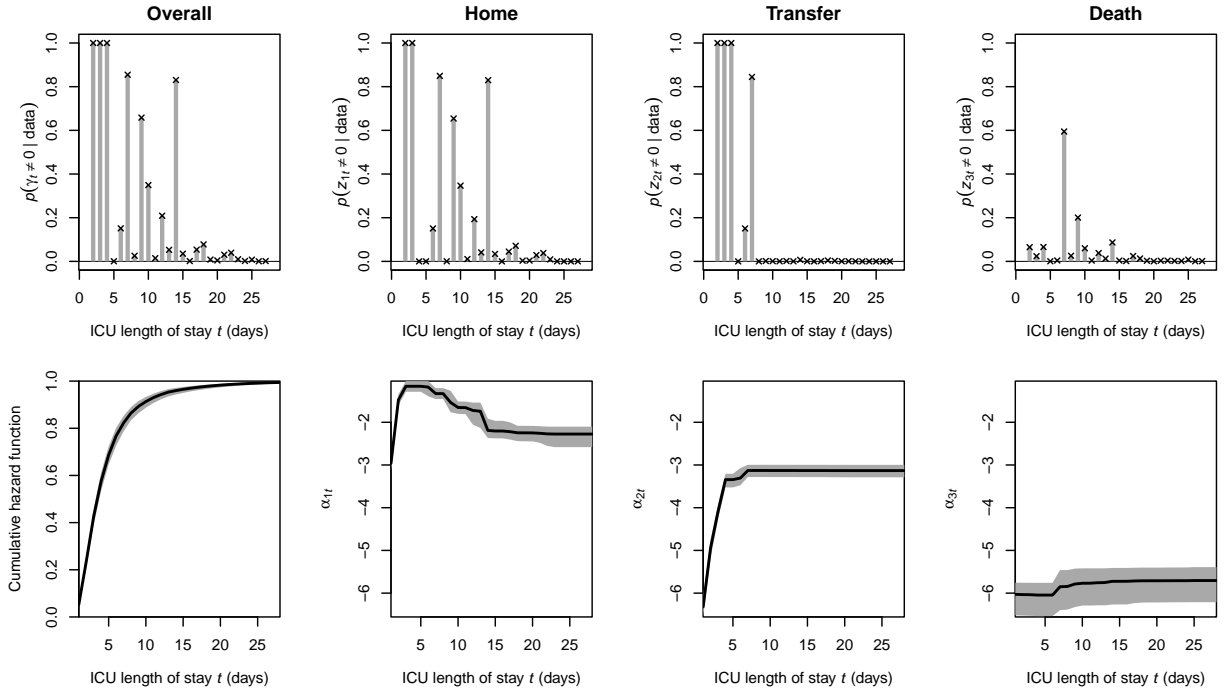


**Figure 3.** ICU data: Posterior inference on the overall (left column) and cause-specific (other columns) baseline hazards. The top row displays the posterior probabilities for the presence of a change point. The bottom row shows posterior inference for the cumulative hazard function for  $\mathbf{x}_i = \mathbf{0}$ , and the baseline hazard parameter  $\alpha_{rt}$ . Black lines represent posterior means and shaded areas correspond to 95% credible intervals.

### 3.2 Posterior inference on the baseline hazards

The posterior probability of absence of overall change points is zero as well as the Bayes factor (see Web Appendix C). Figure 3 summarizes inference on the baseline hazards (see Web Figure 15 for corresponding Bayes factors). The hazard functions differ markedly between risks: the hazard of discharge to home is high in the first two weeks, but not on the first day in the ICU. The hazard of a transfer to another medical facility is lowest during the first few days. Finally, the hazard function for in-hospital mortality does not vary substantially across the length of stay.



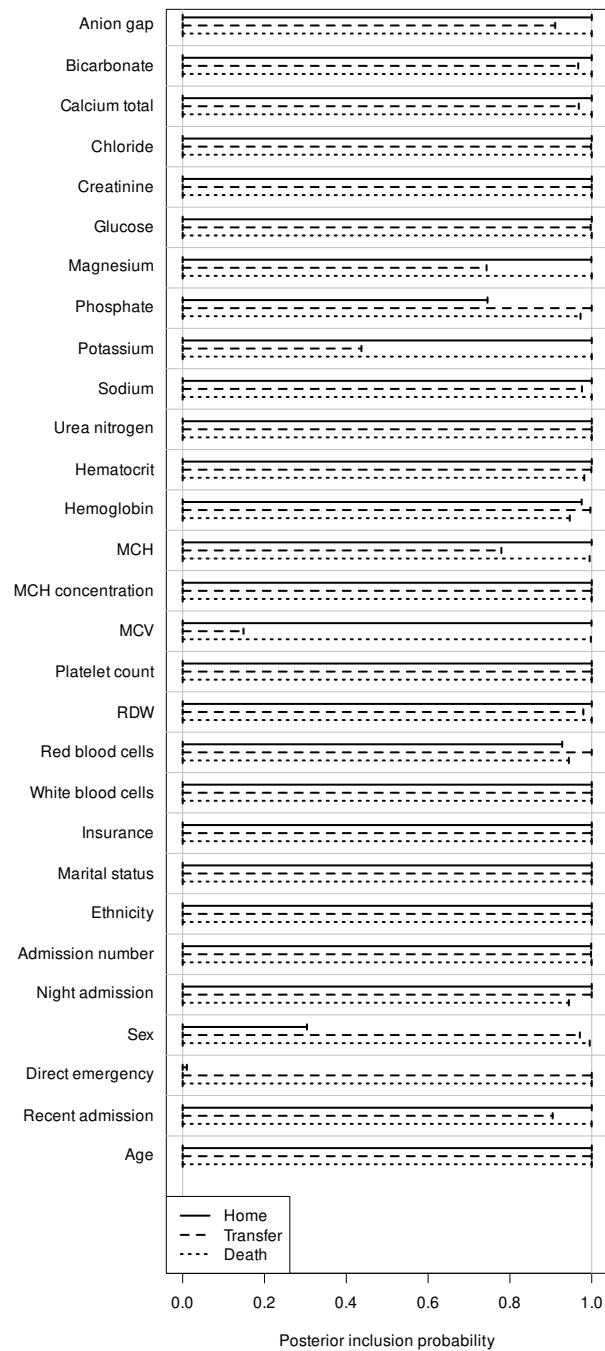


**Figure 4.** ICU data: Posterior inclusion probabilities for each covariate and risk. MCH stands for mean cell hemoglobin, MCV for mean corpuscular volume and RDW for red blood cell distribution width.

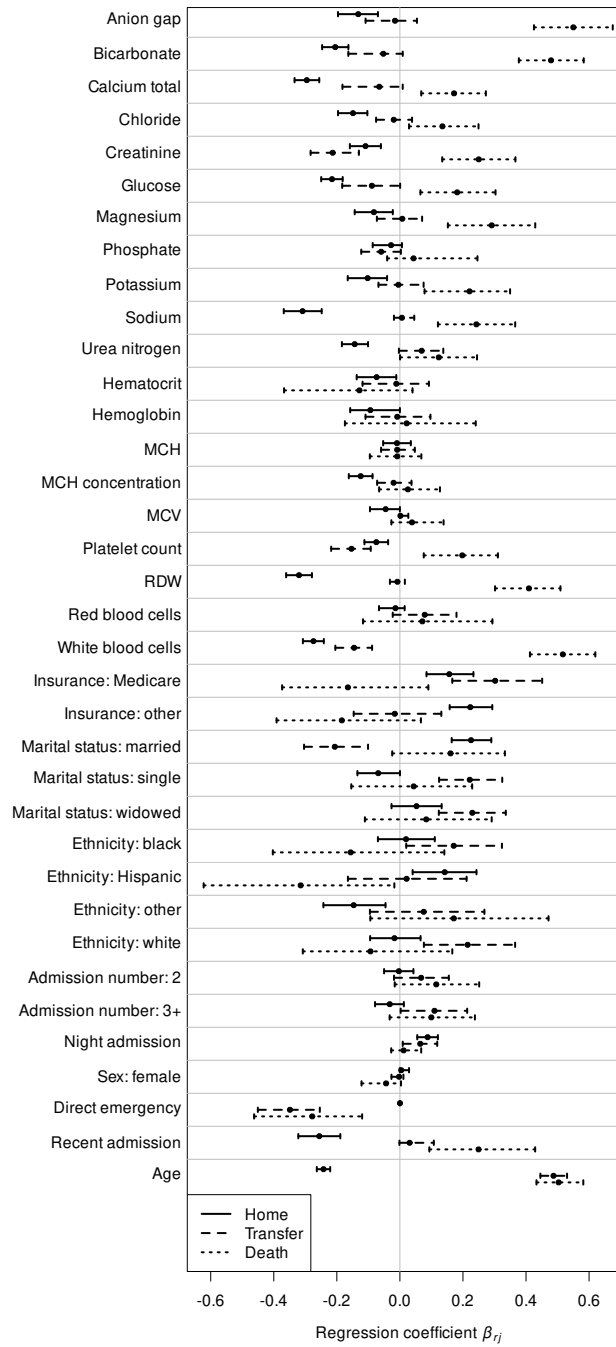


**Figure 5.** ICU data: Posterior means (dot) and 95% credible intervals (lines) of the regression coefficients for each risk. The categorical predictors are coded as dummy variables as detailed in Web Appendix A. MCH stands for mean cell hemoglobin, MCV for mean corpuscular volume and RDW for red blood cell distribution width.

### 3.3 Posterior inference on the regression coefficients

The regression coefficients  $\beta_{rj}$  capture cause-specific covariate effects on length of stay. The spike-and-slab prior provides explicit inference on whether there is a covariate effect through the posterior probability of  $\beta_{rj} \neq 0$ . Posterior inclusion probabilities for each risk are shown in Figure 4. In Figure 5, we report posterior inference on regression coefficients. Finally, we remark that the results on the baseline hazards and covariate effects are in line with those obtained in Meir and Gorfine (2023).

## 4. Comparison with other models

We compare our results on the ICU data to those obtained from maximum likelihood estimation and a more recent alternative, namely the model by King and Weiss (2021).

### 4.1 Maximum likelihood estimation

We maximize the likelihood in (1) using the R package `nnet` (Venables and Ripley, 2002) as the likelihood is equivalent to a multinomial logistic regression (Tutz and Schmid, 2016). The resulting inference is shown in Web Figures 16 and 17. Estimates of  $\alpha_t$  are less smooth than for our model, but are otherwise similar. Estimates of  $\beta_r$  are in agreement with ours.

### 4.2 Semi-parametric model by King and Weiss (2021)

We also compare our model with the Bayesian semi-parametric model by King and Weiss (2021), which also involves multiple risk and a flexible model for the hazard function. For simplicity of explanation in what follows, we denote with  $x_{ij}$  a continuous covariate  $j$  for individual  $i$  and with  $d_{ik}$  a dummy variable corresponding to a level of a categorical covariate. King and Weiss (2021) specify a multinomial logit model for discrete survival analysis with competing risks with  $\eta_{irt} = \alpha_{rt} + \sum_{j=1}^{p^c} f_{\beta_{rj}}(x_{ij}) + \sum_{k=1}^{p^d} \beta_{rk} d_{ik}$  where  $p^c$  and  $p^d$  denote the number of continuous and dummy variables, respectively. Moreover,  $\alpha_{tr} = \beta_{0r} + f_{\alpha r}(t)$  for intercepts  $\beta_{0r}$ , and functions  $f_{\alpha r}$  and  $f_{\beta_{rj}}$  which are object of inference. Note that in their

approach, [King and Weiss \(2021\)](#) include every level of a categorical covariate. The functions  $f_{\alpha r}$  and  $f_{\beta r j}$  are inferred using a Gaussian Markov random field prior. For prior specification and parameter choice, we follow the recommendations in Appendix C of [King and Weiss \(2021\)](#) for uninformative priors. We fit the model using the R package `brea` ([King, 2017](#)) using 50000 burn-in MCMC iterations followed by 200000 recorded iterations.

The resulting inference is shown in Web Figures [19](#), [20](#) and [21](#). The estimates of baseline hazards are in line with our model, though not as smooth. The non-linear covariate effect of age is consistent with the linear effect from our model, but positive association of age and transfer hazard only appears at an older age. The other covariate effects are also similar to the results from our model. See [Figure 5](#).

## 5. Discussion

In this work, we focus on the estimation of the hazard function of competing risks in the context of discrete survival. We assume a change point model for the hazard function, with cause-specific change points, introducing dependence among change point locations across risks. In our approach, both number and location of change points are random. We refer to our model as Multivariate Bernoulli detector. Dependence across risks provides an attractive way for regularization of baseline hazards since changes to an individual's condition across time might affect multiple cause-specific hazards simultaneously. Our approach is widely applicable and interpretable. The data augmentation enables the use of any prior on regression coefficients making the MCMC updates more efficient. The simulation study and the real data application show that posterior inference on change points with dependence across risks is effective, with favorable comparisons with a frequentist approach and the Bayesian semi-parametric model by [King and Weiss \(2021\)](#).

The proposed model can be easily extended to accommodate more complex scenarios, for example, inclusion of recurrent event processes as outcome (see, e.g., [King and Weiss,](#)

2021), of time-varying covariates or semi-competing risk structure. In this work, we employ the multinomial logit model which is a popular choice for the analysis of discrete competing risks. It closely relates to multinomial logistic regression and offers computational advantages. Nevertheless, the Multivariate Bernoulli detector can be used with other likelihoods, such as multinomial probit models or multiple time series. Finally, we note that we could apply the same computational strategy even for change points models in continuous time by restricting the split points to the locations of the events.

#### ACKNOWLEDGEMENTS

This work is supported by the Singapore Ministry of Health’s National Medical Research Council under its Open Fund - Young Individual Research Grant (OFYIRG19nov-0010). A.G. has been partially supported by MUR - Prin 2022 - Grant no. 2022CLTYP4, funded by the European Union - Next Generation EU.

#### SUPPLEMENTARY MATERIALS

Web Appendices and Figures referenced in Sections 2, 3 and 4 are available within this paper’s Supplementary Materials. The code to implement the model is available at <https://github.com/willemvandenboom/mvb-detector>.

#### DATA AVAILABILITY STATEMENT

The data that support the findings of this study are available from PhysioNet. Restrictions apply to the availability of these data, which were used under license for this study. Data are available at [physionet.org](https://physionet.org) with the permission of PhysioNet.

## REFERENCES

- Allison, P. D. (1982). Discrete-time methods for the analysis of event histories. *Sociological Methodology* **13**, 61–98.
- Andersen, P. K., Borgan, Ø., Gill, R. D., and Keiding, N. (1993). *Statistical Models Based on Counting Processes*. Springer Series in Statistics. Springer, New York, NY.
- Andersen, P. K., Geskus, R. B., de Witte, T., and Putter, H. (2012). Competing risks in epidemiology: Possibilities and pitfalls. *International Journal of Epidemiology* **41**, 861–870.
- Bhadra, A., Datta, J., Polson, N. G., and Willard, B. (2019). Lasso meets horseshoe: A survey. *Statistical Science* **34**, 405–427.
- Creswell, R., Lambert, B., Lei, C. L., Robinson, M., and Gavaghan, D. (2020). Using flexible noise models to avoid noise model misspecification in inference of differential equation time series models. arXiv:2011.04854v1.
- Dahl, D. B. (2005). Sequentially-allocated merge-split sampler for conjugate and nonconjugate Dirichlet process mixture models. Technical report, Department of Statistics, Texas A&M University.
- Dickey, J. M. (1971). The weighted likelihood ratio, linear hypotheses on normal location parameters. *The Annals of Mathematical Statistics* **42**, 204–223.
- Dobigeon, N., Tourneret, J.-Y., and Davy, M. (2007). Joint segmentation of piecewise constant autoregressive processes by using a hierarchical model and a Bayesian sampling approach. *IEEE Transactions on Signal Processing* **55**, 1251–1263.
- Fahrmeir, L. and Wagenpfeil, S. (1996). Smoothing hazard functions and time-varying effects in discrete duration and competing risks models. *Journal of the American Statistical Association* **91**, 1584–1594.
- Frühwirth-Schnatter, S. and Frühwirth, R. (2007). Auxiliary mixture sampling with appli-

- cations to logistic models. *Computational Statistics & Data Analysis* **51**, 3509–3528.
- Frühwirth-Schnatter, S. and Frühwirth, R. (2010). Data augmentation and MCMC for binary and multinomial logit models. In Kneib, T. and Tutz, G., editors, *Statistical Modelling and Regression Structures*, pages 111–132. Springer-Verlag, Berlin, Germany.
- Gamerman, D. (1991). Dynamic Bayesian models for survival data. *Journal of the Royal Statistical Society Series C: Applied Statistics* **40**, 63–79.
- Goodman, M. S., Li, Y., and Tiwari, R. C. (2011). Detecting multiple change points in piecewise constant hazard functions. *Journal of Applied Statistics* **38**, 2523–2532.
- Harlé, F., Chatelain, F., Gouy-Pailler, C., and Achard, S. (2016). Bayesian model for multiple change-points detection in multivariate time series. *IEEE Transactions on Signal Processing* **64**, 4351–4362.
- Held, L. and Holmes, C. C. (2006). Bayesian auxiliary variable models for binary and multinomial regression. *Bayesian Analysis* **1**, 145–168.
- Heyard, R., Timsit, J.-F., Essaïed, W. I., and Held, L. (2019). Dynamic clinical prediction models for discrete time-to-event data with competing risks—A case study on the OUTCOMEREA database. *Biometrical Journal* **61**, 514–534.
- Hougaard, P. (1986). Survival models for heterogeneous populations derived from stable distributions. *Biometrika* **73**, 387–396.
- Hougaard, P. (1995). Frailty models for survival data. *Lifetime Data Analysis* **1**, 255–273.
- Hougaard, P., Myglegaard, P., and Borch-Johnsen, K. (1994). Heterogeneity models of disease susceptibility, with application to diabetic nephropathy. *Biometrics* **50**, 1178–1188.
- Johnson, A. E. W., Bulgarelli, L., Shen, L., Gayles, A., Shammout, A., Horng, S., et al. (2023). MIMIC-IV, a freely accessible electronic health record dataset. *Scientific Data* **10**, 1.

- Kalbfleisch, J. D. and Prentice, R. L. (2002). *The Statistical Analysis of Failure Time Data*. John Wiley & Sons, Hoboken, NJ, 2nd edition.
- King, A. J. (2017). brea: Bayesian recurrent event analysis. R package version 0.2.0. <https://CRAN.R-project.org/package=brea>.
- King, A. J. and Weiss, R. E. (2021). A general semiparametric Bayesian discrete-time recurrent events model. *Biostatistics* **22**, 266–282.
- Kozumi, H. (2000). Bayesian analysis of discrete survival data with a hidden Markov chain. *Biometrics* **56**, 1002–1006.
- Landau, V. A. and Zachmann, L. J. (2019). tvgeom: an R package for the time-varying geometric distribution. R package version 1.0.1. <https://CRAN.R-project.org/package=tvgeom>.
- Lee, M., Feuer, E. J., and Fine, J. P. (2018). On the analysis of discrete time competing risks data. *Biometrics* **74**, 1468–1481.
- Linderman, S., Johnson, M. J., and Adams, R. P. (2015). Dependent multinomial models made easy: Stick-breaking with the Pólya-gamma augmentation. In Cortes, C., Lawrence, N., Lee, D., Sugiyama, M., and Garnett, R., editors, *Advances in Neural Information Processing Systems*, volume 28. Curran Associates, Inc.
- Luo, S., Kong, X., and Nie, T. (2016). Spline based survival model for credit risk modeling. *European Journal of Operational Research* **253**, 869–879.
- Mandelbaum, M., Hlynka, M., and Brill, P. H. (2007). Nonhomogeneous geometric distributions with relations to birth and death processes. *TOP* **15**, 281–296.
- Martínez, A. F. and Mena, R. H. (2014). On a nonparametric change point detection model in Markovian regimes. *Bayesian Analysis* **9**, 823–858.
- Matthews, D. E. and Farewell, V. T. (1982). On testing for a constant hazard against a change-point alternative. *Biometrics* **38**, 463–468.



- McFadden, D. (1974). Conditional logit analysis of qualitative choice behavior. In Zarembka, P., editor, *Frontiers in Econometrics, Economic Theory and Mathematical Economics*, pages 105–142. Academic Press, New York, NY.
- Meir, T. and Gorfine, M. (2023). Discrete-time competing-risks regression with or without penalization. arXiv:2303.01186v2.
- Mitchell, T. J. and Beauchamp, J. J. (1988). Bayesian variable selection in linear regression. *Journal of the American Statistical Association* **83**, 1023–1032.
- Möst, S., Pöbnecker, W., and Tutz, G. (2016). Variable selection for discrete competing risks models. *Quality & Quantity* **50**, 1589–1610.
- Polson, N. G., Scott, J. G., and Windle, J. (2013). Bayesian inference for logistic models using Pólya–Gamma latent variables. *Journal of the American Statistical Association* **108**, 1339–1349.
- Polson, N. G. and Sokolov, V. (2019). Bayesian regularization: From Tikhonov to horseshoe. *WIREs Computational Statistics* **11**, e1463.
- Samsonov, S., Lagutin, E., Gabrié, M., Durmus, A., Naumov, A., and Moulines, E. (2022). Local-global MCMC kernels: The best of both worlds. arXiv:2111.02702v3.
- Schmid, M. and Berger, M. (2020). Competing risks analysis for discrete time-to-event data. *WIREs Computational Statistics* **13**, e1529.
- Teugels, J. L. (1990). Some representations of the multivariate Bernoulli and binomial distributions. *Journal of Multivariate Analysis* **32**, 256–268.
- Tutz, G. (1995). Competing risks models in discrete time with nominal or ordinal categories of response. *Quality and Quantity* **29**, 405–420.
- Tutz, G. and Schmid, M. (2016). *Modeling Discrete Time-to-Event Data*. Springer Series in Statistics. Springer, Switzerland.
- Vallejos, C. A. and Steel, M. F. J. (2017). Bayesian survival modelling of university outcomes.

*Journal of the Royal Statistical Society: Series A (Statistics in Society)* **180**, 613–631.

Venables, W. N. and Ripley, B. D. (2002). *Modern Applied Statistics with S*. Statistics and Computing. Springer, New York, NY, 4th edition.

Verdinelli, I. and Wasserman, L. (1995). Computing Bayes factors using a generalization of the Savage-Dickey density ratio. *Journal of the American Statistical Association* **90**, 614–618.

Wang, C.-P. and Ghosh, M. (2007). Change-point diagnostics in competing risks models: Two posterior predictive p-value approaches. *Test* **16**, 145–171.

Supplementary Materials for  
“The Multivariate Bernoulli detector:  
Change point detection in discrete survival analysis”  
by Willem van den Boom, Maria De Iorio,  
Fang Qian and Alessandra Guglielmi

## Web Appendix A ICU data description

The intensive care unit (ICU) data analyzed in Section 3 of the main manuscript are taken from Meir and Gorfine (2023). The data are from the Medical Information Mart for Intensive Care IV (MIMIC-IV) database version 2.0 (Johnson et al., 2022, 2023) which is available from PhysioNet (Goldberger et al., 2000) at <https://physionet.org/content/mimiciv/2.0>. MIMIC-IV contains critical care data from patients admitted to ICUs at the Beth Israel Deaconess Medical Center, which is a tertiary academic medical centre in Boston, Massachusetts.

The analysis considers ICU stays from 2014 to 2020 with admission type ‘direct emergency’, i.e. hospital admission directly into the ICU, or ‘emergency ward’, i.e. admission to the ICU from the emergency ward. Furthermore, if a patient has multiple ICU stays, then only the

last stay is considered. Ultimately, the data consist of  $n = 25159$  ICU stays. The main causes of termination of ICU stays are discharge to home (17357 stays / 69.0%), transfer to another medical facility (5379 stays / 21.4%) and in-hospital mortality (1529 stays / 6.1%). Furthermore, 1.0% of patients leave the ICU against medical advice, which are considered as censored. Additionally, [Meir and Gorfine \(2023\)](#) censor length of stay at 28 days. In total, 894 stays (3.6%) are censored.

Covariates derive from demographics, variables related to the ICU stay and lab tests. The demographics are (i) standardised age; (ii) sex; (iii) ethnicity; (iv) marital status; (v) insurance type. The variables related to the ICU stay are (i) admission type; (ii) whether the admission occurred at night, i.e. between 8am and 8pm; (iii) whether the patient was also admitted during the previous 30 days (*recent admission*); (iv) the number of emergency admissions for the patient (*admission number*). For instance, the admission number is equal to one if the ICU stay is not a repeat admission and equal to two if it is the patient's second emergency admission. We also include 20 lab measurement that are the most commonly recorded within the first 24 hours after admission. Lab tests are coded as binary variables with 1 indicating an abnormal result and 0 otherwise. Categorical covariates are listed in [Web Table 1](#). Note that *age* is the only continuous covariate. Categorical covariates are included in the regression term through the standard dummy variable representation, fixing a category as baseline (see [Web Table 1](#)). This results in  $p = 36$  predictors. Summary statistics of the data are presented in [Tables 4 and 5 of Meir and Gorfine \(2023\)](#).

## Web Appendix B Groupwise variable selection prior

As discussed above, most of the available covariates are categorical, some of which characterised by more than two levels, e.g. *ethnicity*. When performing variable selection, we aim to either keep all the dummy variables corresponding to the same categorical covariate in the model or to exclude all of them. Specifically, let  $S_l$  denote the set of dummy variables corresponding to

Web Table 1: Categorical covariates.

<b>Covariate</b>	<b>Baseline</b>	<b>Other categories</b>			
Demographics					
<i>Sex</i>	Male	Female			
<i>Ethnicity</i>	Asian	White	Black	Hispanic	Other
<i>Marital status</i>	Divorced	Single	Married	Widowed	
<i>Insurance type</i>	Medicaid	Medicare	Other		
Related to ICU stay					
<i>Admission type</i>	Emergency ward	Direct emergency			
<i>Night admission</i>	No	Yes			
<i>Recent admission</i>	No	Yes			
<i>Admission number</i>	1	2	3 or more		
Lab tests					
<i>Anion gap</i>	Normal	Abnormal			
<i>Bicarbonate</i>	Normal	Abnormal			
<i>Calcium total</i>	Normal	Abnormal			
<i>Chloride</i>	Normal	Abnormal			
<i>Creatinine</i>	Normal	Abnormal			
<i>Glucose</i>	Normal	Abnormal			
<i>Magnesium</i>	Normal	Abnormal			
<i>Phosphate</i>	Normal	Abnormal			
<i>Potassium</i>	Normal	Abnormal			
<i>Sodium</i>	Normal	Abnormal			
<i>Urea nitrogen</i>	Normal	Abnormal			
<i>Hematocrit</i>	Normal	Abnormal			
<i>Hemoglobin</i>	Normal	Abnormal			
<i>MCH</i>	Normal	Abnormal			
<i>MCH concentration</i>	Normal	Abnormal			
<i>MCV</i>	Normal	Abnormal			
<i>Platelet count</i>	Normal	Abnormal			
<i>RDW</i>	Normal	Abnormal			
<i>Red blood cells</i>	Normal	Abnormal			
<i>White blood cells</i>	Normal	Abnormal			

MCH stands for mean cell hemoglobin, MCV for mean corpuscular volume and RDW for red blood cell distribution width.

categorical covariate  $l$ . We propose the following modification of the prior on the corresponding regression coefficients from Section 2.4 for groupwise variable selection.

Let  $p_l = |S_l|$  and let  $\boldsymbol{\beta}_{rS_l}$  denote the  $p_l$ -dimensional subvector of  $\boldsymbol{\beta}_r$  corresponding to variables in  $S_l$ . For each risk  $r$  and group  $l$  independently, we assume

$$\boldsymbol{\beta}_{rS_l} \sim \pi_\beta \mathcal{N}_{p_l}(\mathbf{0}, \sigma_\beta^2 I_{p_l}) + (1 - \pi_\beta) \delta_{\mathbf{0}}$$

where  $\mathcal{N}_{p_l}(\mathbf{0}, \sigma_\beta^2 I_{p_l})$  is a  $p_l$ -dimensional Gaussian distribution with mean zero and covariance matrix  $\sigma_\beta^2 I_{p_l}$ ,  $\mathbf{0}$  is the zero vector and  $\delta_{\mathbf{0}}$  denotes a point mass at  $\mathbf{0}$ . Thus, a priori, the elements of  $\boldsymbol{\beta}_{rS_l}$  are all non-zero (resp. zero) simultaneously with probability  $\pi_\beta$  (resp.  $1 - \pi_\beta$ ). The hyperprior on  $\pi_\pi$  remains  $\pi_\beta \sim \mathcal{U}(0, 1)$  as in Section 2.4 of the main manuscript.

## Web Appendix C Bayes factor for change points

We now describe a strategy to test for the presence of change points. In particular, we provide a strategy to compute the Bayes factor  $B$  for  $K = 0$  (model  $\mathcal{M}^*$ , denoting no change points) versus a model with  $K \sim p(K)$  (model  $\mathcal{M}$ ) (see Legramanti, Rigon, and Durante, 2022, for a similar example of such model comparison).  $B$  is readily computed from Markov chain Monte Carlo (MCMC) output. Let  $\mathbf{y}$  denote all the observed data. Then

$$B = \frac{p(\mathbf{y} | \mathcal{M}^*)}{p(\mathbf{y} | \mathcal{M})} = \frac{p(\mathbf{y} | K = 0)}{p(\mathbf{y})} = \frac{p(\mathbf{y}, K = 0)}{p(\mathbf{y}) p(K = 0)} = \frac{p(K = 0 | \mathbf{y})}{p(K = 0)}$$

where the last ratio is the Savage-Dickey ratio (Dickey, 1971; Verdinelli and Wasserman, 1995). Here,  $p(K = 0 | \mathbf{y})$  is readily estimated by the MCMC sample frequency of  $K = 0$  while  $p(K = 0)$  is available from the prior.

The scheme can be employed as long as  $p(K = 0)$  is not too small as it would lead to unstable estimation of  $B$  when also  $p(K = 0 | \mathbf{y})$  is small (i.e. the MCMC chain visits

$K = 0$  only rarely). This is not the case in our scenario as  $K \sim \text{Geo}_{|\mathcal{T}|}(\pi_K)$  such that  $p(K = 0) > \pi_K = 0.5$ .

## Web Appendix D Local-global MCMC algorithm

Here, we provide further details on the MCMC, including the data augmentation from [Frühwirth-Schnatter and Frühwirth \(2007\)](#), and the methodology from Bayesian nonparametrics based on [Dahl \(2005\)](#), [Martínez and Mena \(2014\)](#) and [Creswell et al. \(2020\)](#).

Let  $\boldsymbol{\theta} = (\theta_1, \dots, \theta_n)$ . Let  $\mathbf{y}$  denote all the observed data. Then, the likelihood for all observations is

$$p(\mathbf{y} \mid \boldsymbol{\theta}) = \prod_{i=1}^n \left[ \lambda_{r_i}(t_i \mid \theta_i)^{\delta_i} \prod_{l=1}^{t_i - \delta_i} \{1 - \lambda(l \mid \theta_i)\} \right] \quad (\text{D1})$$

### D.1 Local MCMC with data augmentation

For the data augmentation, we consider the following Gaussian mixture approximation of the standard Gumbel density:  $\exp(-u - e^{-u}) \approx \sum_{c=1}^{10} w_c \mathcal{N}(u \mid \xi_c, s_c^2)$  where the weights  $w_c$ , means  $\xi_c$  and variances  $s_c^2$  of each component  $c$  are given in Table 1 of [Frühwirth-Schnatter and Frühwirth \(2007\)](#). Conditionally on the linear predictors  $\eta_{irt}$ , we sample the augmented data, consisting of a latent variable  $u_{irt}$  and a component indicator  $c_{irt}$ , according to Step (b) in Section 3.2 of [Frühwirth-Schnatter and Frühwirth \(2007\)](#) as detailed in Algorithm D1. Then, the augmented likelihood follows as

$$p(\mathbf{y} \mid \mathbf{u}, \mathbf{c}, \boldsymbol{\theta}) = \prod_{r=1}^m \prod_{i=1}^n \prod_{l=1}^{t_i} \mathcal{N}(u_{irl} \mid \eta_{irl} + \xi_{c_{irl}}, s_{c_{irl}}^2)$$

Its Gaussianity enables convenient MCMC updates for the parameters constituting  $\boldsymbol{\theta}$ .

Firstly, we perform a split-merge-shuffle step based on [Martínez and Mena \(2014\)](#) to update  $\gamma_t$  with  $\alpha_{r\ell}^*$  integrated out from the augmented likelihood. Here, *split* refers to the addition

---

**Algorithm D1** Sampling of the augmented data  $u_{irt}$  and  $c_{irt}$ .

---

For  $i = 1, \dots, n$ ; for  $l = 1, \dots, t_i$ :

1. Sample  $U_{il} \sim \mathcal{U}(0, 1)$ .
2. For  $r = 1, \dots, m$ , sample  $V_{irl} \sim \mathcal{U}(0, 1)$  and set

$$u_{irt} = -\log \left\{ -\frac{\log(U_{il})}{1 + \sum_{\rho=1}^m \exp(\eta_{i\rho l})} - \mathbb{1} \left[ \begin{array}{l} l \neq t_i \\ \text{or } \delta_i = 0 \\ \text{or } r_i \neq r \end{array} \right] \frac{\log(V_{irl})}{\exp(\eta_{irl})} \right\}$$

3. Sample  $c_{irl} \in \{1, \dots, 10\}$  according to

$$P(c_{irl} = c) \propto \frac{w_c}{s_c} \exp \left\{ -\frac{1}{2s_c^2} (u_{irt} - \eta_{irl} - \xi_c)^2 \right\}$$

---

of an overall change point that splits a time interval, i.e. constant baseline hazard, into two. *Merge* refers to the deletion of a change point that merges two adjacent time intervals. Lastly, a *shuffle* is the relocation of a change point such that the lengths of its adjacent time intervals change.

For the description of the MCMC step, we introduce additional notation. The overall change points marked by  $\gamma_t$  partition the time points  $\{1, \dots, t_{\max}\}$  into  $K + 1$  time intervals. Denote the number of time points in the  $\ell$ -th time interval by  $n_\ell$ . Due to conjugacy, we can integrate out  $\alpha_{rt}$  from the augmented likelihood to obtain a closed form expression for  $p(\mathbf{y} \mid \mathbf{u}, \mathbf{c}, \boldsymbol{\theta} \setminus \boldsymbol{\alpha}) = p(\mathbf{y} \mid \mathbf{u}, \mathbf{c}, \boldsymbol{\zeta})$  where  $\boldsymbol{\zeta} = \boldsymbol{\theta} \setminus \boldsymbol{\alpha}$  only consists of change point indicators and regression coefficients. We detail the split-merge-shuffle step in Algorithm D2.

Metropolis-Hastings steps for  $\mathbf{z}_t$ ,  $\alpha_{r\ell}^*$  and  $\boldsymbol{\beta}_r$  follow from the Gaussian augmented likelihood as detailed in Algorithms D3, D4 and D5, respectively. We state the update for  $\boldsymbol{\beta}_r$  in Algorithm D5 for the groupwise variable selection prior in Web Appendix B. The update for the non-grouped prior in Section 2.4 of the main manuscript can be obtained by assigning each predictor to its own group  $S_l$ , i.e.  $S_l = \{l\}$  for  $l = 1, \dots, p$ .



---

**Algorithm D2** Split-merge-shuffle step for  $\gamma_t$  based on the augmented likelihood.

---

1. Perform a split or a merge step:

- (a) With probability  $\mathbf{1}[K = 0] + \frac{1}{2}\mathbf{1}[0 < K < t_{\max} - 1]$ , perform a split step:
- i. Sample a time interval  $\ell'$  uniformly from  $\{\ell \mid n_\ell \geq 2\}$ .
  - ii. Split time interval  $\ell'$  by setting  $\gamma_{t'} = 1$  for a  $t'$  sampled uniformly from  $\{2 + \sum_{\kappa=1}^{\ell'-1} n_\kappa, 3 + \sum_{\kappa=1}^{\ell'-1} n_\kappa, \dots, \sum_{\kappa=1}^{\ell'} n_\kappa\}$ .
  - iii. Sample corresponding cause-specific change points  $\mathbf{z}'_{t'}$  from the prior  $p(\mathbf{z}_{t'} \mid \gamma_{t'})$ . Let  $\zeta'$  denote the resulting parameter where the other change points and  $\beta_r$  are left unchanged.
  - iv. Set  $\zeta = \zeta'$  with probability

$$\min \left\{ 1, \frac{2^{\mathbf{1}[K > 0]} |\{\ell \mid n_\ell \geq 2\}| (n_{\ell'} - 1) p(\zeta') p(\mathbf{y} \mid \mathbf{u}, \mathbf{c}, \zeta')}{2^{\mathbf{1}[K < t_{\max} - 2]} (K + 1) p(\mathbf{z}'_{t'} \mid \gamma_{t'}) p(\zeta) p(\mathbf{y} \mid \mathbf{u}, \mathbf{c}, \zeta)} \right\}$$

(b) Otherwise, perform a merge step:

- i. Sample a time interval  $\ell'$  uniformly from  $\{1, \dots, K\}$ .
- ii. Let  $\zeta'$  denote the parameter resulting from merging time intervals  $\ell'$  and  $(\ell' + 1)$ , and the corresponding removal of change points.
- iii. Let  $t_{\text{old}} = 1 + \sum_{\kappa=1}^{\ell'} n_\kappa$ . Set  $\zeta = \zeta'$  with probability

$$\min \left\{ 1, \frac{2^{\mathbf{1}[K < t_{\max} - 1]} K p(\mathbf{z}_{t_{\text{old}}} \mid \gamma_{t_{\text{old}}}) p(\zeta') p(\mathbf{y} \mid \mathbf{u}, \mathbf{c}, \zeta')}{2^{\mathbf{1}[K > 1]} |\{\ell \mid n'_\ell \geq 2\}| (n'_{\ell'} - 1) p(\zeta) p(\mathbf{y} \mid \mathbf{u}, \mathbf{c}, \zeta)} \right\}$$

where  $n'_{\ell'}$  is the duration of the merged time interval.

2. If  $K > 0$ , perform a shuffle step:

- (a) Sample a time interval  $\ell'$  uniformly from  $\{1, \dots, K\}$ . Let  $t_{\text{old}} = 1 + \sum_{\kappa=1}^{\ell'} n_\kappa$ .
- (b) Sample a new overall change point  $t'$  uniformly from  $\{t_{\text{old}} - n_{\ell'}, t_{\text{old}} - n_{\ell'} + 1, \dots, t_{\text{old}} + n_{\ell'+1} - 1\}$ .
- (c) Let  $\zeta'$  denote the parameter resulting from setting  $\gamma'_{t'} = 1$ ,  $\mathbf{z}'_{t'} = \mathbf{z}_{t_{\text{old}}}$  and, if  $t' \neq t_{\text{old}}$ ,  $\gamma'_{t_{\text{old}}} = 0$  and  $\mathbf{z}_{t_{\text{old}}} = \mathbf{0}$ .
- (d) Set  $\zeta = \zeta'$  with probability

$$\min \left\{ 1, \frac{p(\zeta') p(\mathbf{y} \mid \mathbf{u}, \mathbf{c}, \zeta')}{p(\zeta) p(\mathbf{y} \mid \mathbf{u}, \mathbf{c}, \zeta)} \right\}$$


---

---

**Algorithm D3** Metropolis-Hastings step for  $\mathbf{z}_t$  based on the augmented likelihood.

---

If  $K > 0$ , update  $\mathbf{z}_t$  corresponding to a randomly sampled time interval:

1. Sample  $\ell'$  uniformly from  $\{2, \dots, K + 1\}$ . Let  $t' = 1 + \sum_{\kappa=1}^{\ell'-1} n_\kappa$ .
2. Sample cause-specific change points  $\mathbf{z}'_{t'}$  from the prior  $p(\mathbf{z}_{t'} | \gamma_{t'})$ . Let  $\boldsymbol{\zeta}'$  denote the resulting parameter where the other change points and  $\boldsymbol{\beta}_r$  are left unchanged.
3. Set  $\boldsymbol{\zeta} = \boldsymbol{\zeta}'$  with probability

$$\min \left\{ 1, \frac{p(\mathbf{y} | \mathbf{u}, \mathbf{c}, \boldsymbol{\zeta}')}{p(\mathbf{y} | \mathbf{u}, \mathbf{c}, \boldsymbol{\zeta})} \right\}$$


---

**Algorithm D4** Gibbs sampling step for  $\alpha_{r\ell}^*$  based on the augmented likelihood.

---

For  $r = 1, \dots, m$ , update  $\alpha_{r\ell}^*$ :

1. Let  $S_\ell^r = \{t \mid \ell - 1 \leq \sum_{l=2}^t z_{rl} < \ell\}$  denote the set of times in the  $\ell$ -th cause-specific time interval for competing risk  $r$ .
2. For  $\ell = 1, \dots, 1 + \sum_{l=2}^{t_{\max}} z_{rl}$ , sample  $\alpha_{r\ell}^* = \alpha_{rt}$ ,  $t \in S_\ell^r$ , corresponding to the  $\ell$ -th time interval from its full conditional:

$$\alpha_{r\ell}^* | \mathbf{u}, \mathbf{c}, \boldsymbol{\zeta} \sim \mathcal{N} \left\{ \sigma_{\alpha r\ell}^2 \left( \frac{\mu_\alpha}{\sigma_\alpha^2} + \sum_{l \in S_\ell^r} \sum_{\{i \mid l \leq t_i\}} \frac{u_{irl} - \xi_{c_{irl}}}{s_{c_{irl}}^2} \right), \sigma_{\alpha r\ell}^2 \right\}$$

where  $\sigma_{\alpha r\ell}^2 = 1/(1/\sigma_\alpha^2 + 1/\sum_{l \in S_\ell^r} \sum_{\{i \mid l \leq t_i\}} s_{c_{irl}}^2)$ .

---

## D.2 Global MCMC from Bayesian nonparametrics

In the data augmentation, the latent variables  $\mathbf{u}$  and component indicators  $\mathbf{c}$  can strongly reflect the values for  $\boldsymbol{\alpha}_t$  associated with the current change point configuration. Therefore, we also consider MCMC updates for the change point indicators  $\gamma_t$  and  $\mathbf{z}_t$  that directly use the unaugmented likelihood in (D1). The updates are detailed in Algorithms D6 and D7. They closely mirror Algorithms D2 and D3, respectively, which use the augmented likelihood. The main difference is that values need to be proposed for  $\boldsymbol{\alpha}_t$  as it is not integrated out from the likelihood here.

---

**Algorithm D5** MCMC step for  $\pi_\beta$  and  $\beta_1, \dots, \beta_m$  based on the augmented likelihood.

---

1. Recall from Web Appendix B that  $S_l$  denotes a group of predictors. Let  $B_r^* = \{l \mid \beta_{rS_l} \neq \mathbf{0}\}$  and  $b_r^* = |B_r^*|$  denote the indices and the number, respectively, of non-zero groups of coefficients in  $\beta_r$ . Sample

$$\pi_\beta \mid \beta_1, \dots, \beta_m \sim \text{Beta} \left\{ 1 + \sum_{r=1}^m b_r^*, 1 + \sum_{r=1}^m (L - b_r^*) \right\}$$

where  $L$  is the number of groups of predictors.

2. For  $r = 1, \dots, m$ , update  $\beta_r$  similarly to Section 2.5 of [Held and Holmes \(2006\)](#):
  - (a) Let  $B_r = \{j \mid \beta_{rj} \neq 0\}$  and  $b_r = |B_r|$  denote the indices and the number, respectively, of non-zero elements in  $\beta_r$ . Also, let  $\Sigma_{B_r} = \{I_{b_r}/\sigma_\beta^2 + \sum_{i=1}^n \sum_{l=1}^{t_i} \mathbf{x}_{iB_r} \mathbf{x}_{iB_r}^\top / s_{c_{ir}l}^2\}^{-1}$  where  $\mathbf{x}_{iB_r}$  is the  $b_r$ -dimensional subvector of  $\mathbf{x}_i = (x_{i1}, \dots, x_{ip})$  indexed by  $B_r$ , and  $\boldsymbol{\mu}_{B_r} = \Sigma_{B_r} \sum_{i=1}^n \mathbf{x}_{iB_r} \sum_{l=1}^{t_i} (u_{irl} - \xi_{c_{ir}l} - \alpha_{rl}) / s_{c_{ir}l}^2$ .
  - (b) Update the set  $B_r^*$ , i.e. which groups of predictors are included. For  $l = 1, \dots, L$ :
    - i. Construct a Metropolis-Hastings proposal  $B_r^{*'}$  from  $B_r^*$  by adding  $l$  to  $B_r^*$  if  $l \in B_r^*$  and removing  $l$  from  $B_r^*$  otherwise. Let  $b_r^{*'} = |B_r^{*'}|$ . Based on the proposal  $B_r^{*'}$ , we define  $B_r'$  and  $b_r'$  analogously to  $B_r$  and  $b_r$ .
    - ii. Set  $B_r^* = B_r^{*'}$  with probability

$$\min \left\{ 1, \frac{|\Sigma_{B_r'}|^{1/2} \sigma_\beta^{b_r} \exp(\boldsymbol{\mu}_{B_r'}^\top \Sigma_{B_r'}^{-1} \boldsymbol{\mu}_{B_r'} / 2) \pi_\beta^{b_r^{*'} - b_r^*}}{|\Sigma_{B_r}|^{1/2} \sigma_\beta^{b_r'} \exp(\boldsymbol{\mu}_{B_r}^\top \Sigma_{B_r}^{-1} \boldsymbol{\mu}_{B_r} / 2) (1 - \pi_\beta)^{b_r^{*'} - b_r^*}} \right\}$$

- (c) Set  $\beta_{rj} = 0$  for  $j \notin B_r$  and sample

$$\beta_{rB_r} \mid B_r, \mathbf{u}, \mathbf{c}, \boldsymbol{\alpha}_1, \dots, \boldsymbol{\alpha}_{t_{\max}} \sim \mathcal{N}(\boldsymbol{\mu}_{B_r}, \Sigma_{B_r})$$


---

---

**Algorithm D6** Split-merge-shuffle step for  $\gamma_t$  based on the unaugmented likelihood.

---

1. Perform a split or a merge step:

(a) With probability  $\mathbf{1}[K = 0] + \frac{1}{2}\mathbf{1}[0 < K < t_{\max} - 1]$ , perform a split step:

- i. Sample a time interval  $\ell'$  uniformly from  $\{\ell \mid n_\ell \geq 2\}$ .
- ii. Split time interval  $\ell'$  by setting  $\gamma_{t'} = 1$  for a  $t'$  sampled uniformly from  $\{2 + \sum_{\kappa=1}^{\ell'-1} n_\kappa, 3 + \sum_{\kappa=1}^{\ell'-1} n_\kappa, \dots, \sum_{\kappa=1}^{\ell'} n_\kappa\}$ .
- iii. Sample corresponding cause-specific change points  $\mathbf{z}'_{t'}$  from the prior  $p(\mathbf{z}'_{t'} \mid \gamma_{t'})$ .
- iv. For each newly introduced cause-specific change point, propose values  $\alpha_{r,\ell'+1}^{\star'}$  for  $t$  corresponding to the newly introduced time interval by sampling from  $\mathcal{N}(\alpha_{r,\ell'}^{\star}, 1)$ . Let  $\boldsymbol{\theta}'$  denote the resulting parameter where the other change points, the other  $\boldsymbol{\alpha}_t$  and  $\boldsymbol{\beta}_r$  are left unchanged.
- v. Set  $\boldsymbol{\theta} = \boldsymbol{\theta}'$  with probability

$$\min \left\{ 1, \frac{2^{\mathbf{1}[K>0]} |\{\ell \mid n_\ell \geq 2\}| (n_{\ell'} - 1) p(\boldsymbol{\theta}') p(\mathbf{y} \mid \boldsymbol{\theta}')}{2^{\mathbf{1}[K < t_{\max} - 2]} (K + 1) p(\mathbf{z}'_{t'} \mid \gamma_{t'}) p(\boldsymbol{\theta}) p(\mathbf{y} \mid \boldsymbol{\theta}) \prod_{\{r \mid z'_{rt'} = 1\}} \mathcal{N}(\alpha_{r,\ell'+1}^{\star'} \mid \alpha_{r,\ell'}^{\star}, 1)} \right\}$$

(b) Otherwise, perform a merge step:

- i. Sample a time interval  $\ell'$  uniformly from  $\{1, \dots, K\}$ .
- ii. Let  $\boldsymbol{\theta}'$  denote the parameter resulting from merging time intervals  $\ell'$  and  $(\ell' + 1)$ , and the corresponding removal of change points. Here, the baseline hazards  $\alpha_{r,\ell'}^{\star}$  from time interval  $\ell'$  are used for the merged time interval while the  $\alpha_{r,\ell'+1}^{\star}$  from time interval  $(\ell' + 1)$  are discarded.
- iii. Let  $t_{\text{old}} = 1 + \sum_{\kappa=1}^{\ell'} n_\kappa$ . Set  $\boldsymbol{\theta} = \boldsymbol{\theta}'$  with probability

$$\min \left\{ 1, \frac{2^{\mathbf{1}[K < t_{\max} - 1]} K p(\mathbf{z}_{t_{\text{old}}} \mid \gamma_{t_{\text{old}}}) p(\boldsymbol{\theta}') p(\mathbf{y} \mid \boldsymbol{\theta}') \prod_{\{r \mid z_{rt_{\text{old}}} = 1\}} \mathcal{N}(\alpha_{r,\ell'+1}^{\star} \mid \alpha_{r,\ell'}^{\star}, 1)}{2^{\mathbf{1}[K > 1]} |\{\ell \mid n'_\ell \geq 2\}| (n'_{\ell'} - 1) p(\boldsymbol{\theta}) p(\mathbf{y} \mid \boldsymbol{\theta})} \right\}$$

where  $n'_{\ell'}$  is the duration of the merged time interval.

2. If  $K > 0$ , perform a shuffle step:

- (a) Sample a time interval  $\ell'$  uniformly from  $\{1, \dots, K\}$ . Let  $t_{\text{old}} = 1 + \sum_{\kappa=1}^{\ell'} n_\kappa$ .
- (b) Sample a new overall change point  $t'$  uniformly from

$$\{t_{\text{old}} - n_{\ell'}, t_{\text{old}} - n_{\ell'} + 1, \dots, t_{\text{old}} + n_{\ell'+1} - 1\}.$$

- (c) Let  $\boldsymbol{\theta}'$  denote the parameter resulting from setting  $\gamma'_{t'} = 1$ ,  $\mathbf{z}'_{t'} = \mathbf{z}_{t_{\text{old}}}$  and, if  $t' \neq t_{\text{old}}$ ,  $\gamma'_{t_{\text{old}}} = 0$  and  $\mathbf{z}_{t_{\text{old}}} = \mathbf{0}$ , while leaving the baseline hazards  $\alpha_{r\ell}^*$  corresponding to each time interval the same. That is, only the duration of the time intervals change.
- (d) Set  $\boldsymbol{\theta} = \boldsymbol{\theta}'$  with probability

$$\min \left\{ 1, \frac{p(\boldsymbol{\theta}') p(\mathbf{y} | \boldsymbol{\theta}')}{p(\boldsymbol{\theta}) p(\mathbf{y} | \boldsymbol{\theta})} \right\}$$

---

We are now ready to state the full MCMC step used for the Multivariate Bernoulli detector in Algorithm D8. The computationally most expensive part is typically Step 1a which samples the augmented data using Algorithm D1. More precisely, Step 3 of Algorithm D1 is most expensive. Fortunately, it is embarrassingly parallel across individuals  $i$  and times  $l$  such that its computation can be readily sped up using multicore computing. In the global step, the unaugmented likelihood  $p(\mathbf{y} | \boldsymbol{\theta})$  in (D1) can also be expensive to compute. See Section 4.1.3 and Appendix A of King and Weiss (2021) for ways to speed up evaluation of such a likelihood.

---

**Algorithm D7** Metropolis-Hastings step for  $\mathbf{z}_t$  based on the unaugmented likelihood.

---

If  $K > 0$ , update  $\mathbf{z}_t$  corresponding to a randomly sampled time interval:

1. Sample  $\ell'$  uniformly from  $\{2, \dots, K + 1\}$ . Let  $t' = 1 + \sum_{\kappa=1}^{\ell'-1} n_\ell$ .
2. Sample cause-specific change points  $\mathbf{z}'_{t'}$  from the prior  $p(\mathbf{z}_{t'} | \gamma_{t'})$ .
3. For each newly introduced cause-specific change point (i.e.  $z'_{rt'} = 1$  and  $z_{rt'} = 0$ ), propose values  $\alpha_{r\ell'}^*$  corresponding to the new cause-specific time interval that it starts by sampling from  $\mathcal{N}(\alpha_{r,\ell'-1}^*, 1)$ . For each removed cause-specific change point (i.e.  $z_{rt'} = 1$  and  $z'_{rt'} = 0$ ), carry forward the baseline hazards  $\alpha_{r,\ell'-1}^*$  from time interval  $(\ell' - 1)$  to time interval  $\ell'$ . Let  $\boldsymbol{\theta}'$  denote the resulting parameter where the other change points, the other  $\alpha_{r\ell}^*$  and  $\boldsymbol{\beta}_r$  are left unchanged.
4. Set  $\boldsymbol{\theta} = \boldsymbol{\theta}'$  with probability

$$\min \left\{ 1, \frac{p(\mathbf{z}_{t'} | \gamma_{t'}) p(\boldsymbol{\theta}') p(\mathbf{y} | \boldsymbol{\theta}') \prod_{\{r|z_{rt'}=1 \& z'_{rt'}=0\}} \mathcal{N}(\alpha_{r\ell'}^* | \alpha_{r,\ell'-1}^*, 1)}{p(\mathbf{z}'_{t'} | \gamma_{t'}) p(\boldsymbol{\theta}) p(\mathbf{y} | \boldsymbol{\theta}) \prod_{\{r|z'_{rt'}=1 \& z_{rt'}=0\}} \mathcal{N}(\alpha_{r\ell'}^* | \alpha_{r,\ell'-1}^*, 1)} \right\}$$


---

---

**Algorithm D8** Local-global MCMC step for the Multivariate Bernoulli detector.

---

1. Local step:
    - (a) Sample the data augmentation  $\mathbf{u}$  and  $\mathbf{c}$  per Algorithm D1.
    - (b) Update  $\gamma_t$  and  $\mathbf{z}_t$  using the augmented likelihood per Algorithm D2.
    - (c) Update  $\mathbf{z}_t$  using the augmented likelihood per Algorithm D3.
    - (d) Update  $\boldsymbol{\alpha}_t$  using the augmented likelihood per Algorithm D4.
    - (e) Update  $\boldsymbol{\beta}_1, \dots, \boldsymbol{\beta}_m$  using the augmented likelihood per Algorithm D5.
  2. Global step:
    - (a) Update  $\gamma_t$ ,  $\mathbf{z}_t$  and  $\boldsymbol{\alpha}_t$  using the unaugmented likelihood  $p(\mathbf{y} | \boldsymbol{\theta})$  per Algorithm D6.
    - (b) Update  $\mathbf{z}_t$  and  $\boldsymbol{\alpha}_t$  using the unaugmented likelihood  $p(\mathbf{y} | \boldsymbol{\theta})$  per Algorithm D7.
-

## Web Appendix E Simulation study

Here we present a comprehensive simulation study, which includes a wide variety of scenarios, replicate simulated data sets, and comparisons with maximum likelihood estimation and the model by [King and Weiss \(2021\)](#).

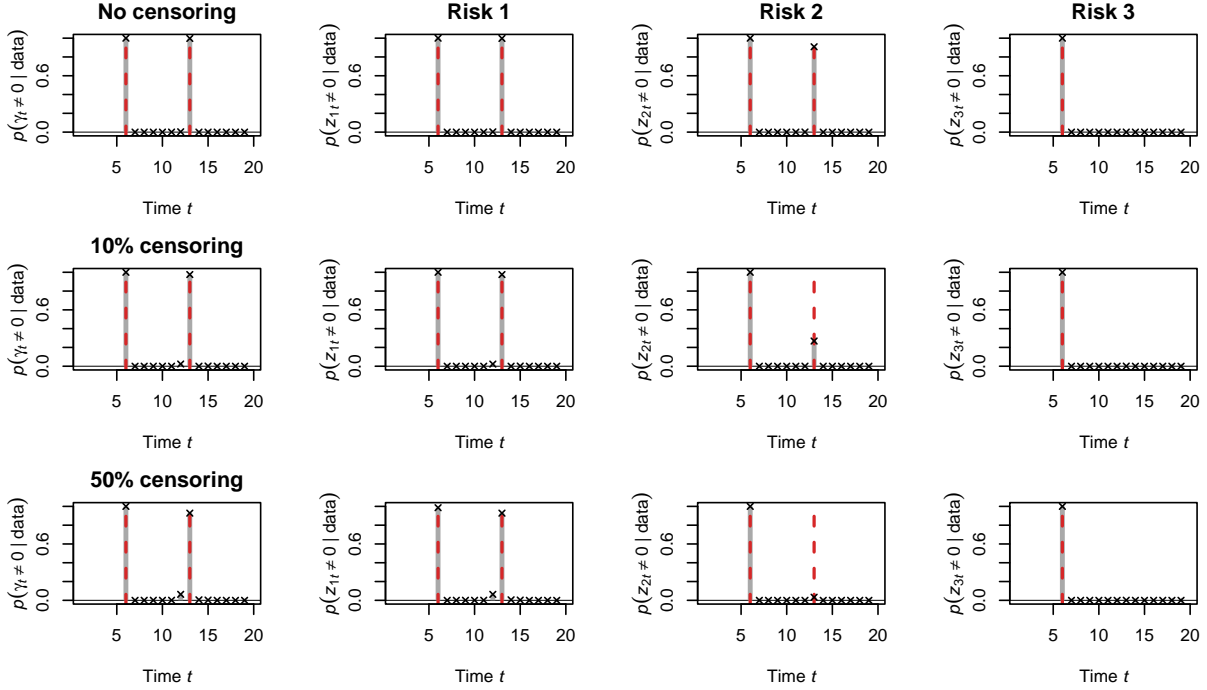
### E.1 Simulation study without change points

We apply the Multivariate Bernoulli detector to data simulated without change points. We simulate  $n = 100$  observations from the model in Section 2 with  $m = 3$  risks, no predictors ( $p = 0$ ), no censoring ( $\delta_i = 1$ ), and constant baseline hazard  $\boldsymbol{\alpha}_t = (-2, -3, -4)$ ,  $t \geq 1$ . We fit our model with  $t_{\max} = \max_i t_i = 26$ . We run the MCMC chain for 100000 iterations, discarding the first 10000 as burn-in.

The MCMC estimate of the posterior probability of no change points is 0.83. Also, the estimate of the Bayes factor of no change points from Web Appendix C is 1.89 which is in line with the absence of change points. Finally, the 95% credible intervals for  $\boldsymbol{\alpha}_t$  are from  $(-2.2, -3.2, -10.4)$  to  $(-1.9, -2.7, -3.4)$  which include the true values  $\boldsymbol{\alpha}_t = (-2, -3, -4)$ .

### E.2 Simulation study with change points

Here, focus is on inference on change points. We simulate  $n = 300$  observations from the model in Section 2 of the main manuscript with  $t_{\max} = 20$ ,  $m = 3$  risks, no covariates ( $p = 0$ ) and baseline hazard with two change points: one at  $t = 6$  involving all three risks and another at  $t = 13$  affecting only risks 1 and 2. Specifically,  $\boldsymbol{\alpha}_t = (-9, -9, -9)$  before the first change point ( $t = 1, \dots, 5$ ),  $\boldsymbol{\alpha}_t = (-4, -3, -3)$  between the two change points ( $t = 6, \dots, 12$ ) and  $\boldsymbol{\alpha}_t = (-2, -2, -3)$  after the second change point ( $t = 13, \dots$ ). We consider three scenarios with (i) no censoring beyond those with  $T_i = t_{\max} + 1$ , and (ii) 10% and (iii) 50% of the individuals being censored, which are selected at random. For those censored individuals, we sample the censoring time  $C_i$  uniformly from the set  $\{1, \dots, T_i - 1\}$ . We fit our model

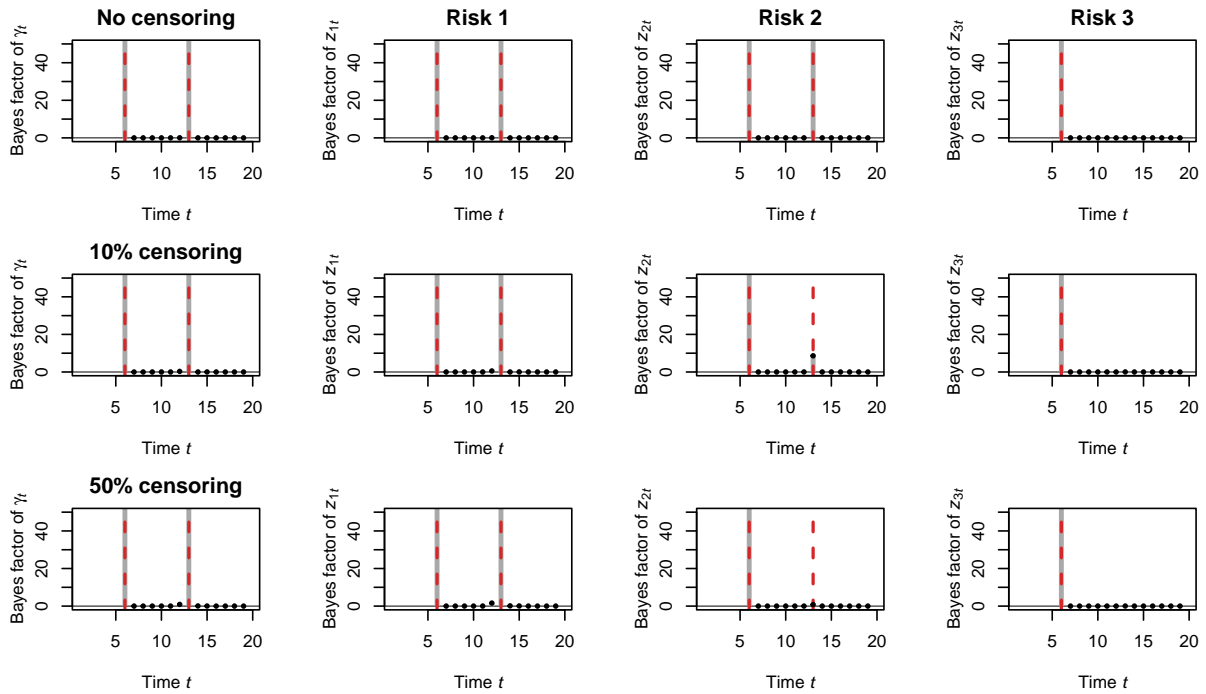


Web Figure 1: Simulation study: Posterior probabilities for the presence of a change point for the overall (left column) and cause-specific (other columns) hazard functions. The gray lines correspond to posterior probabilities. The dashed red lines are drawn in correspondence of the true change points.

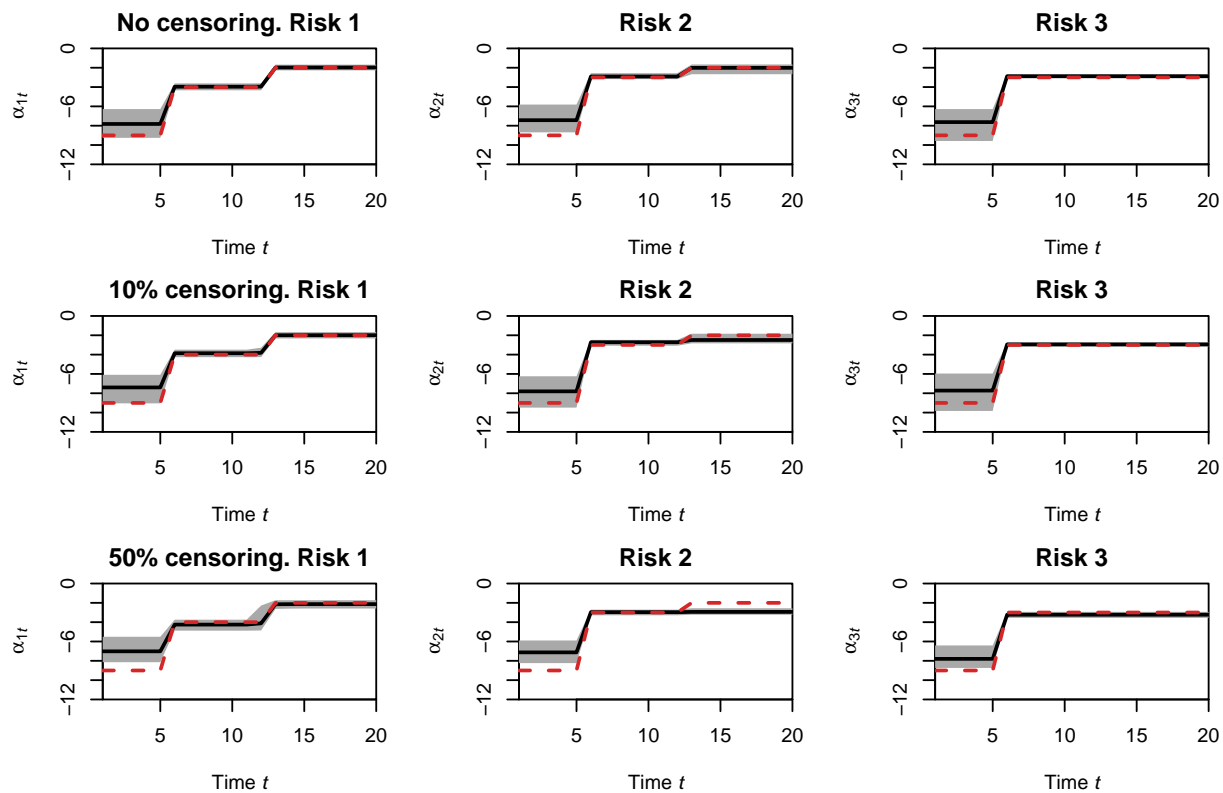
using 100000 MCMC iterations, discarding the first 10000 as burn-in which takes around four minutes with an AMD Ryzen 7950X CPU with a base clock speed of 4.5 GHz.

We summarize the resulting inference on change points in Web Figure 1 using the posterior probabilities of  $\gamma_t = 1$  and  $z_{rt} = 1$  (see Web Figure 2 for corresponding Bayes factors). The values are shown only for those times  $t \in \mathcal{T}$  at which change points are allowed. Our model recovers both the overall and cause-specific change points with high accuracy in the absence of censoring. With 10% censoring, inference on the relatively minor second change point in the second risk is more uncertain. This cause-specific change point is missed with 50% censoring. Inference on  $\alpha_{rt}$ , presented in Web Figure 3, similarly shows accurate recovery across all risks only for scenarios (i) and (ii) with limited censoring. Finally, the estimate of the Bayes factor in Web Appendix C and the posterior probability of no change points are zero in all three scenarios.



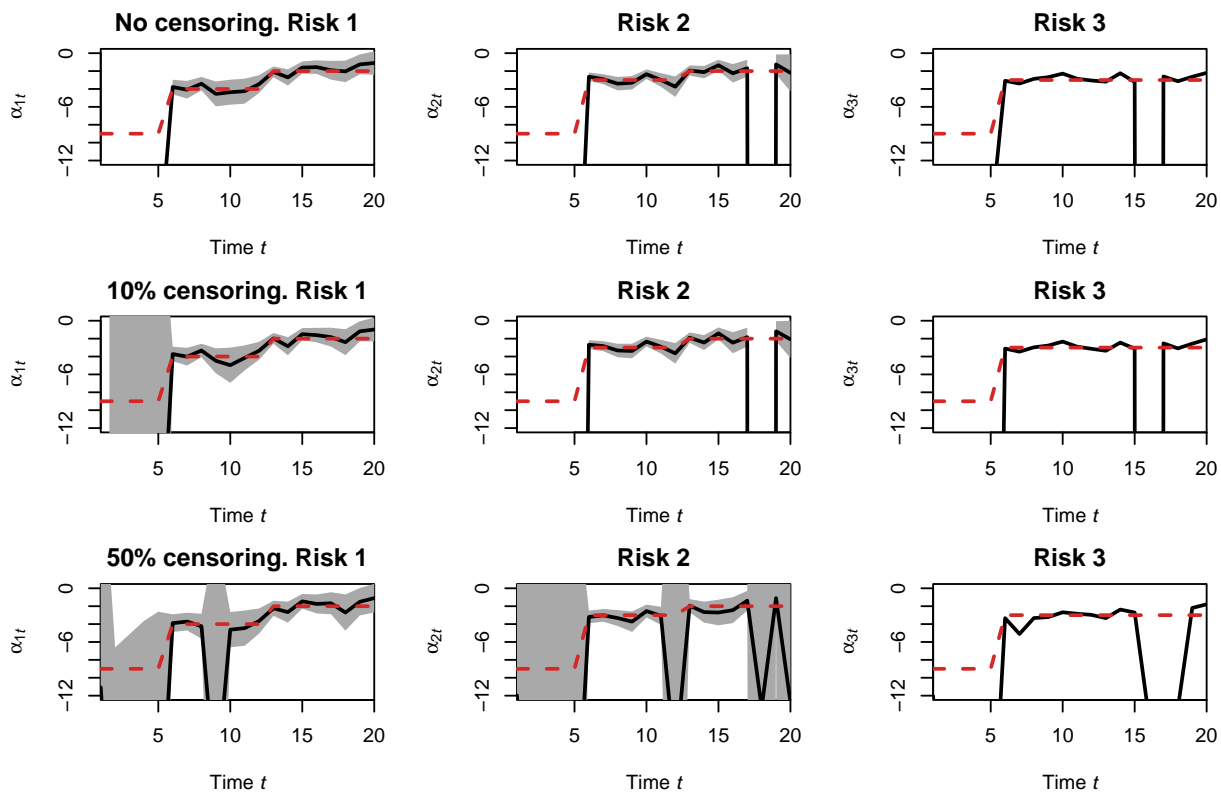


Web Figure 2: Simulation study: Bayes factors for the presence of a change point for the overall (left column) and cause-specific (other columns) hazard functions. The gray lines correspond to Bayes factors, some of which are outside the plotting range. The dashed red lines are drawn in correspondence of the true change points.

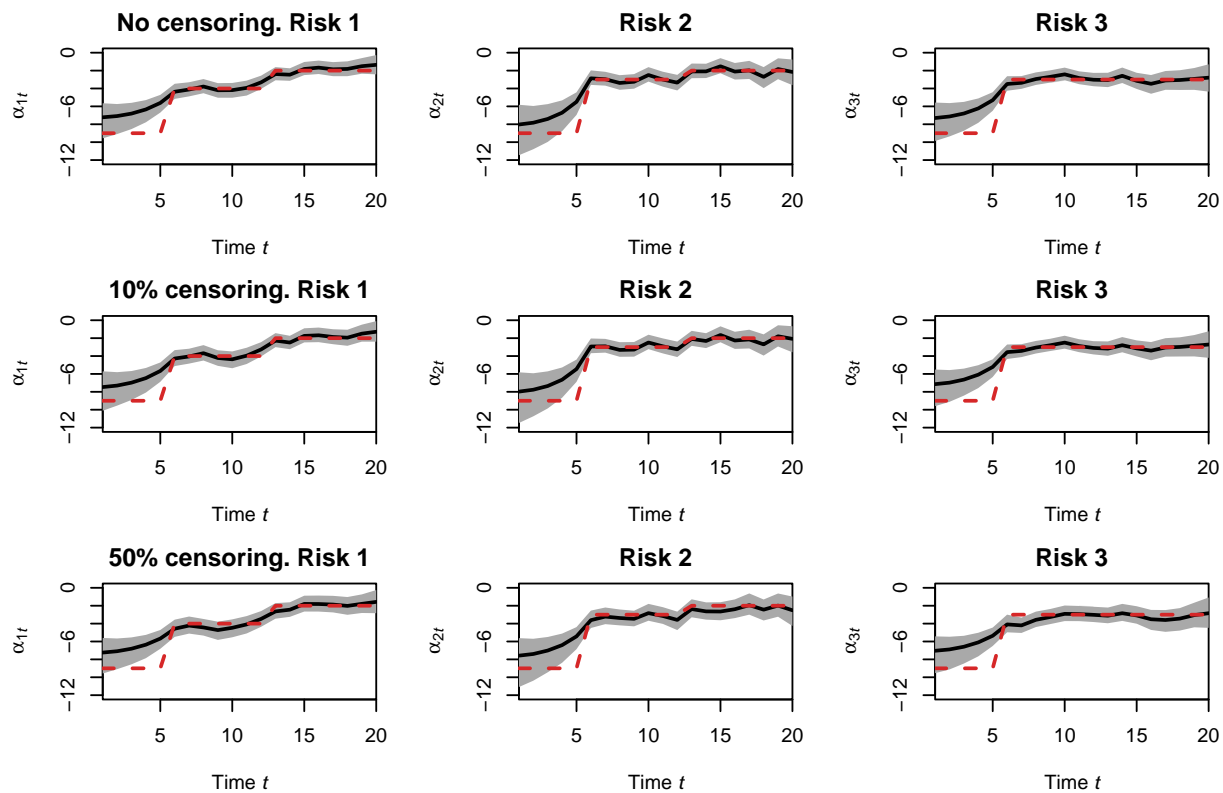


Web Figure 3: Simulation study: Posterior inference on the baseline hazard parameter  $\alpha_{rt}$  from the Multivariate Bernoulli detector. Solid lines represent posterior means and shaded areas correspond to 95% credible intervals. The dashed lines are drawn in correspondence of the true  $\alpha_{rt}$ .

We also fit the models described in Section 4 with results shown in Web Figures 4 and 5. The maximum likelihood estimates are non-smooth and can be far from the true values of  $\alpha_{rt}$ , showing the need for regularization of such estimation. The model by King and Weiss (2021) provides smoother estimates, though with generally wider confidence intervals than the Multivariate Bernoulli detector. A reason for this might be that the Multivariate Bernoulli detector can detect and exploit sharing of information across risks while King and Weiss (2021) smooth each risk independently.



Web Figure 4: Simulation study: Maximum likelihood estimates of the baseline hazard parameter  $\alpha_{rt}$  (solid lines) with their 95% confidence intervals demarcated by shaded areas. The dashed lines are drawn in correspondence of the true  $\alpha_{rt}$ . The confidence interval is not available for some  $\alpha_{rt}$  due to numerical issues.



Web Figure 5: Simulation study: Posterior inference on the baseline hazard parameter  $\alpha_{rt}$  from the model by [King and Weiss \(2021\)](#). Solid lines represent posterior means and shaded areas correspond to 95% credible intervals. The dashed lines are drawn in correspondence of the true  $\alpha_{rt}$ .

## E.3 Simulation study with replicates

### E.3.1 Setup

We consider ten scenarios by varying (i) censoring level; (ii) number of observations  $n$ ; (iii) number of predictors  $p$ ; (iv) number of competing risks  $m$ . The scenarios are detailed in Web Table 2. In all scenarios,  $t_{\max} = 15$  and the baseline hazard has two change points: the first change point is at  $t = 6$  and involves all risks except in scenarios with  $m = 4$  risks when the fourth risk does not have a change point at  $t = 6$ . The second change point is at  $t = 13$  and involves only the first and third risks. Specifically, for scenarios with  $m = 4$ ,

$\boldsymbol{\alpha}_t = (-5, -5, -5, -4)$  before the first change point ( $t = 1, \dots, 5$ ),

$\boldsymbol{\alpha}_t = (-4, -3, -3, -4)$  between the two change points ( $t = 6, \dots, 12$ ) and

$\boldsymbol{\alpha}_t = (-2, -3, -2, -4)$  after the second change point ( $t = 13, \dots$ ). For scenarios with  $m = 2, 3$  risks, the baseline hazard  $\boldsymbol{\alpha}_t$  includes the first two or three elements of the previous vectors.

Regression coefficients  $\beta_{rj}$  and (categorical) predictors  $x_{rj}$  are sampled independently and uniformly from the sets  $\{-0.1, 0, 0.1\}$  and  $\{0, 1\}$ , respectively. Then, data are simulated as in Section E.2. We replicate each scenario 128 times.

For each of the 128 replicate data sets, we fit the Multivariate Bernoulli detector as described in Section E.2. For comparison, we also estimate  $\boldsymbol{\alpha}_t$  and  $\beta_{rj}$  by maximum likelihood, as described in Section 4.1, and fitting the model by King and Weiss (2021), as described in Section 4.2.

### E.3.2 Results

To summarize inference across scenarios and replicates, we focus on mean squared error (MSE) and bias of the estimates for the baseline hazard  $\boldsymbol{\alpha}_t$ , the regression coefficients  $\beta_{rj}$  and the number of change points  $K$ . In addition to  $K = \sum_{t \in \mathcal{T}} \gamma_t$ , we also consider the number of cause-specific change points  $K_r = \sum_{t \in \mathcal{T}} z_{rt}$  where  $z_{rt} = \mathbb{1}[\alpha_{rt} \neq \alpha_{r(t-1)}]$ . The MSE and bias are averaged across time, risks and predictors. In more details, let us denote the estimates of

Web Table 2: Simulation scenarios.

<b>Scenario</b>	<b>Censoring level</b>	$n$	$p$	$m$
<i>Varying censoring level</i>				
i	0%	500	3	2
ii	10%	500	3	2
iii	50%	500	3	2
<i>Varying number of observations</i>				
iv	10%	200	3	2
ii	10%	500	3	2
v	10%	1000	3	2
<i>Varying number of predictors</i>				
ii	10%	500	3	2
vi	10%	500	5	2
<i>Varying number of competing risks with <math>n = 500</math></i>				
ii	10%	500	3	2
vii	10%	500	3	3
viii	10%	500	3	4
<i>Varying number of competing risks with <math>n = 1000</math></i>				
v	10%	1000	3	2
ix	10%	1000	3	3
x	10%	1000	3	4

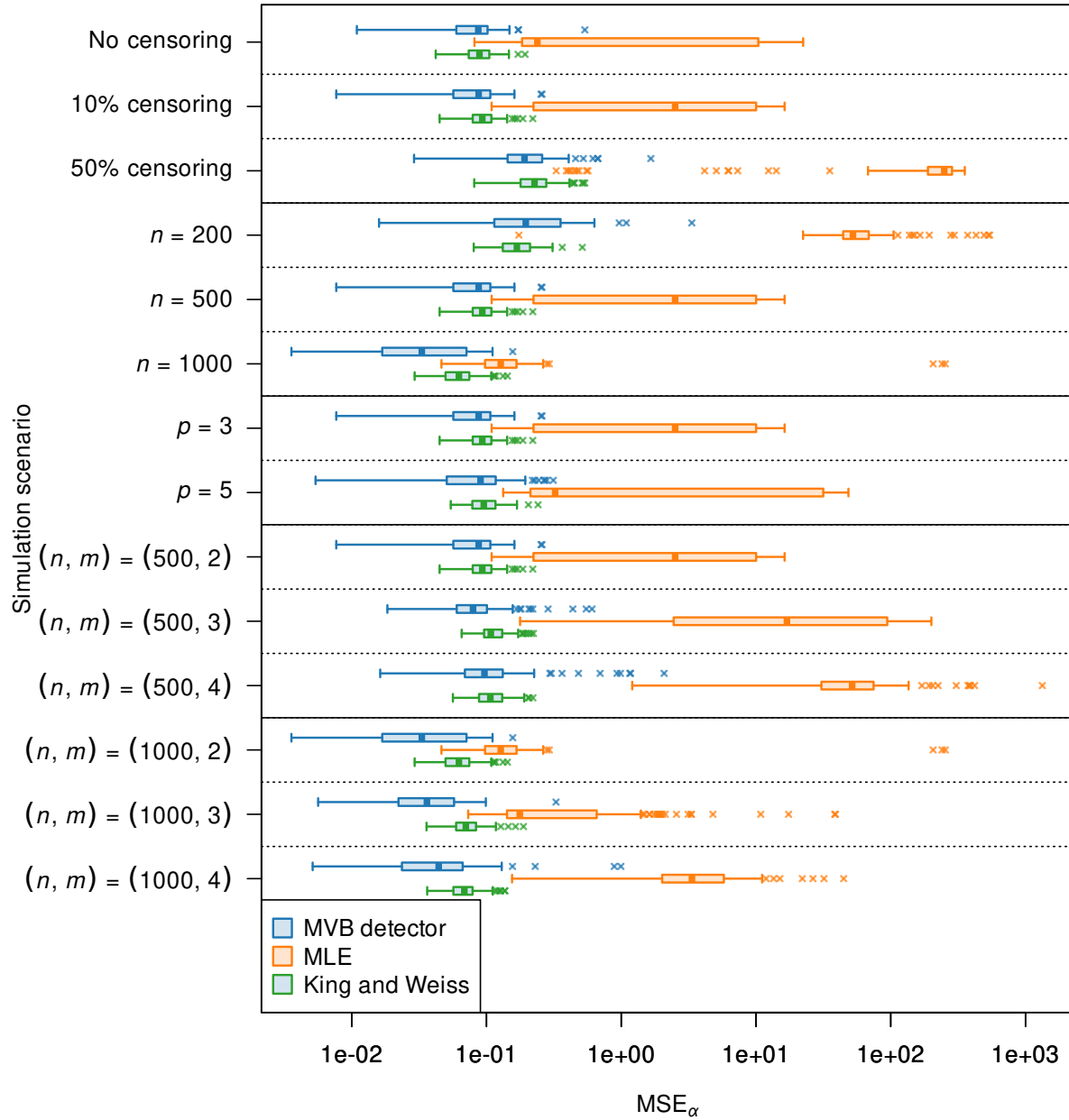
In the table,  $n$  denotes the number of observations,  $p$  the number of predictors and  $m$  the number of competing risks.

the parameters by (i)  $\hat{\alpha}_t$ ; (ii)  $\hat{\beta}_{rj}$ ; (iii)  $\hat{K}$ ; (iv)  $\hat{K}_r$ . Here, the estimates are either the posterior mean or the maximum likelihood estimate. We compute, for each replicate,

$$\begin{aligned} \text{MSE}_\alpha &= \frac{1}{m t_{\max}} \sum_t \sum_r (\hat{\alpha}_{rt} - \alpha_{rt})^2 \\ \text{bias}_\alpha &= \frac{1}{m t_{\max}} \sum_t \sum_r (\hat{\alpha}_{rt} - \alpha_{rt}) \\ \text{MSE}_\beta &= \frac{1}{m p} \sum_j \sum_r (\hat{\beta}_{rj} - \alpha_{rt})^2 \\ \text{bias}_\beta &= \frac{1}{m p} \sum_j \sum_r (\hat{\beta}_{rj} - \alpha_{rt}) \\ \text{MSE}_K &= (\hat{K} - K)^2 \\ \text{bias}_K &= \hat{K} - K \\ \text{MSE}_{K_r} &= \frac{1}{m} \sum_r (\hat{K}_r - K_r)^2 \\ \text{bias}_{K_r} &= \frac{1}{m} \sum_r (\hat{K}_r - K_r) \end{aligned}$$

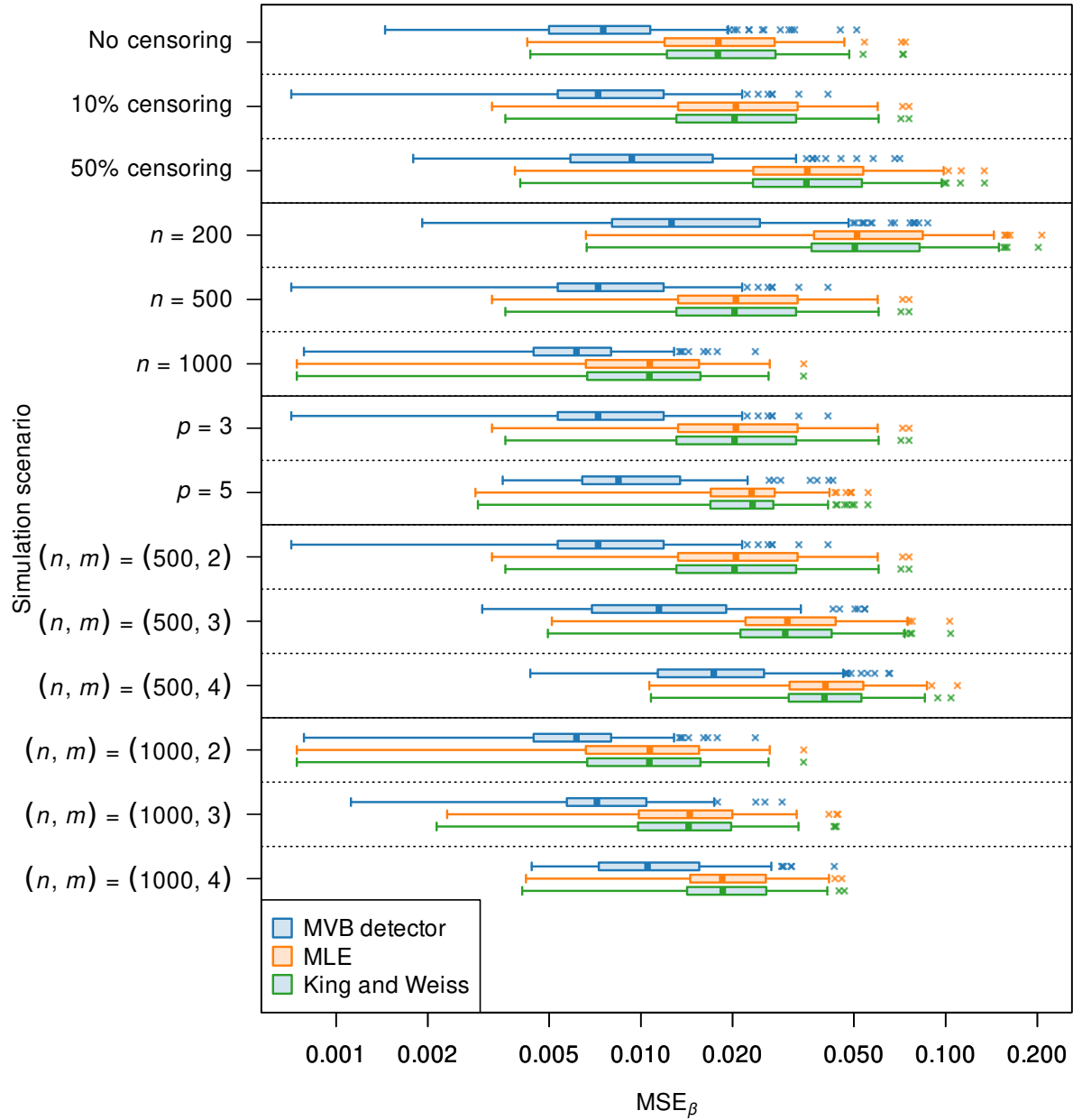
The results are summarized in Web Figures 6 through 11. Note that some scenarios are visualised multiple times in the figures for ease of comparison. In terms of mean squared error, the Multivariate Bernoulli detector outperforms both maximum likelihood estimation and the model by [King and Weiss \(2021\)](#) in almost all scenarios (see Web Figures 6 and 7). Maximum likelihood estimation presents large  $\text{MSE}_\alpha$ , suggesting unstable estimation for the unconstrained approach: we discuss how unconstrained estimation can lead to unstable estimation in Section 1 of the main manuscript.

In terms of bias (see Web Figures 8 and 9), the comparison is more nuanced. For the baseline hazards, maximum likelihood estimation performs the worst with significant underestimation of  $\alpha_t$ . On the other hand, the Multivariate Bernoulli detector and the model by [King](#)

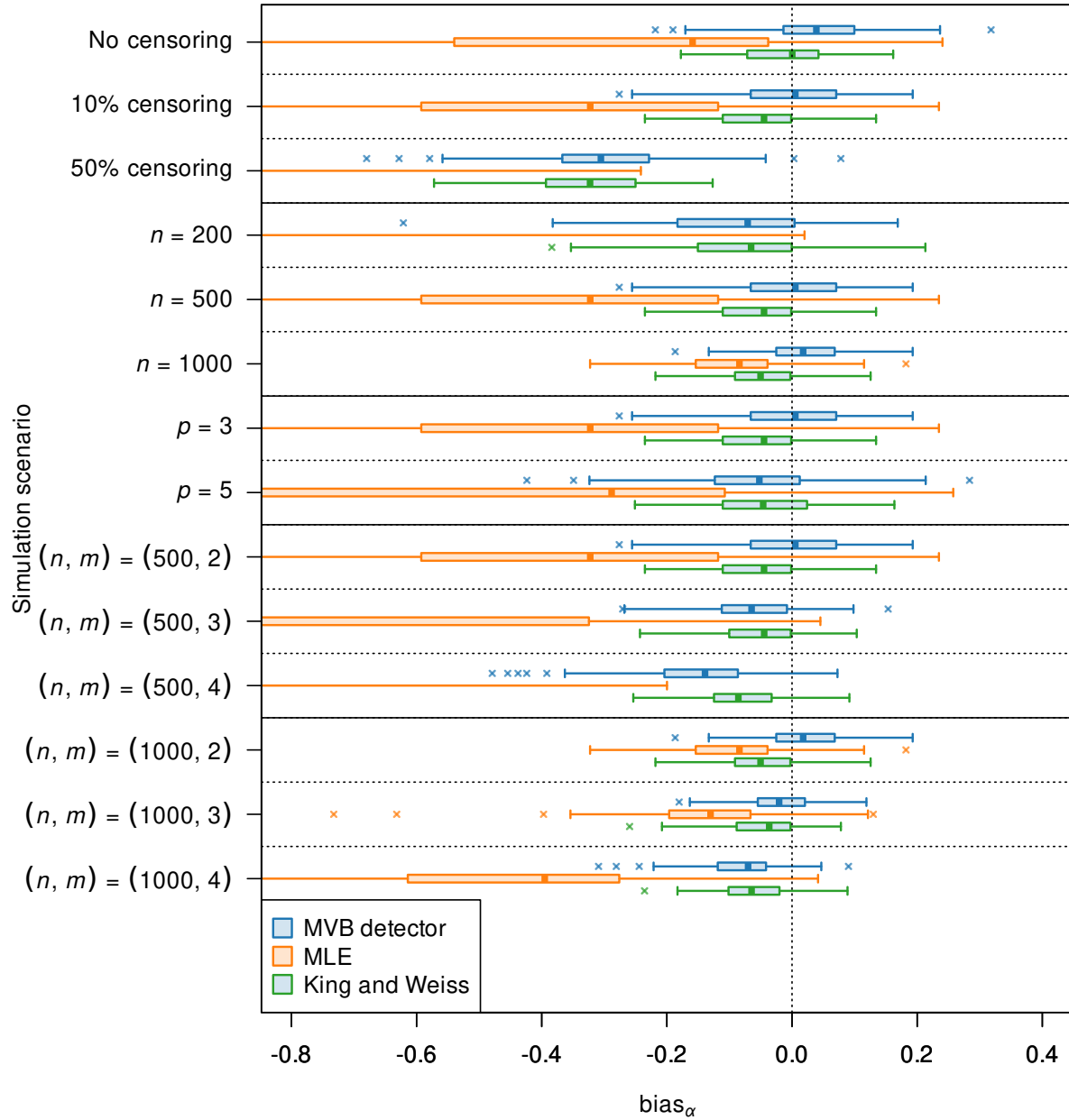


Web Figure 6: Simulation study: For each scenario, we plot the distribution of the mean squared error (MSE) of the inference on the baseline hazard parameter  $\alpha_{rt}$  across the 128 replicates from the Multivariate Bernoulli (MVB) detector, maximum likelihood estimation (MLE) and the model by King and Weiss (2021).

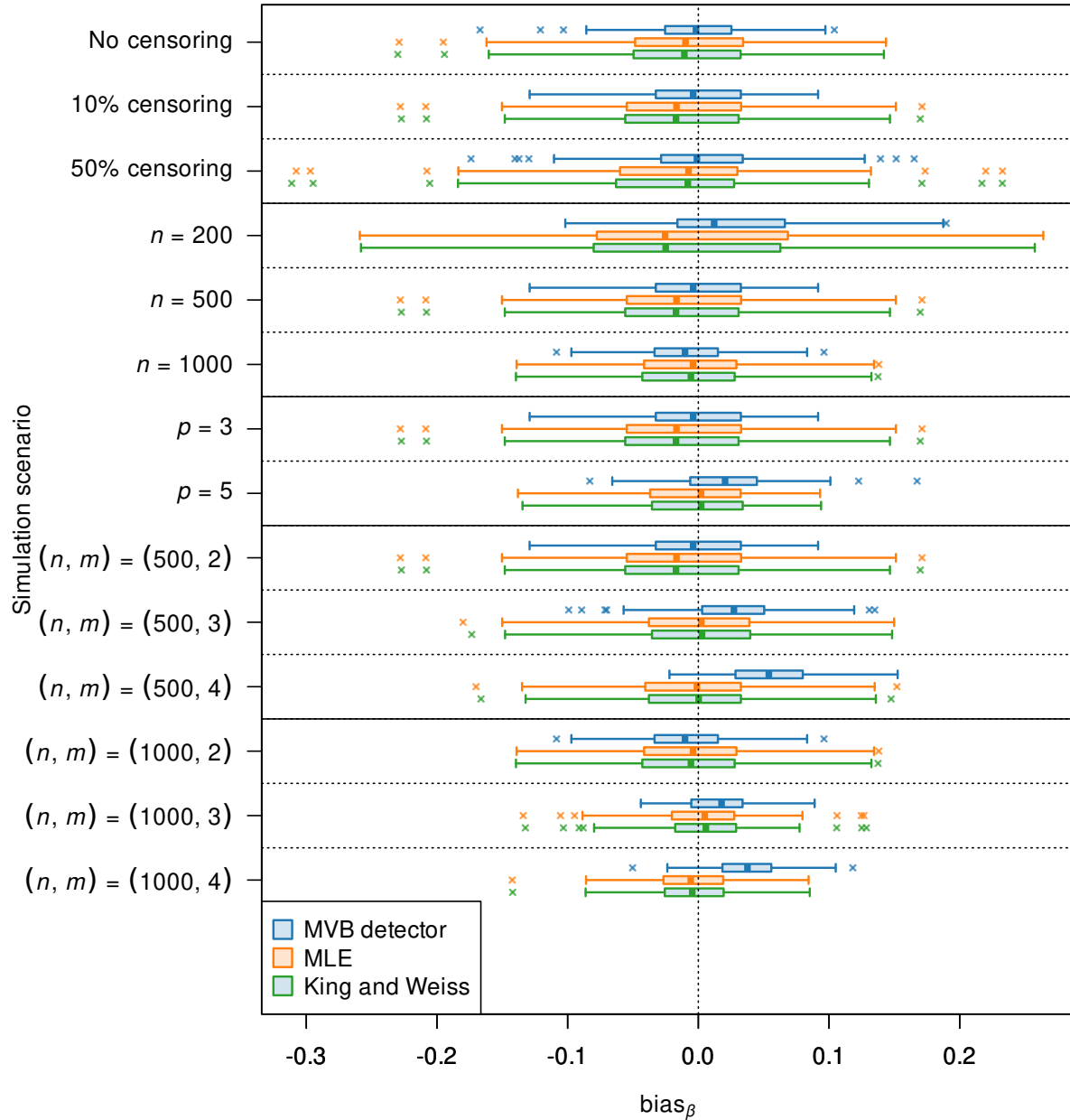




Web Figure 7: Simulation study: For each scenario, we plot the distribution of the mean squared error (MSE) of the inference on the regression coefficients  $\beta_{r_j}$  across the 128 replicates from the Multivariate Bernoulli (MVB) detector, maximum likelihood estimation (MLE) and the model by King and Weiss (2021).



Web Figure 8: Simulation study: For each scenario, we plot the distribution of the average bias of the estimates of the baseline hazard parameter  $\alpha_{rt}$  across the 128 replicates from the Multivariate Bernoulli (MVB) detector, maximum likelihood estimation (MLE) and the model by [King and Weiss \(2021\)](#). Some results for the MLE are outside the plotting range.



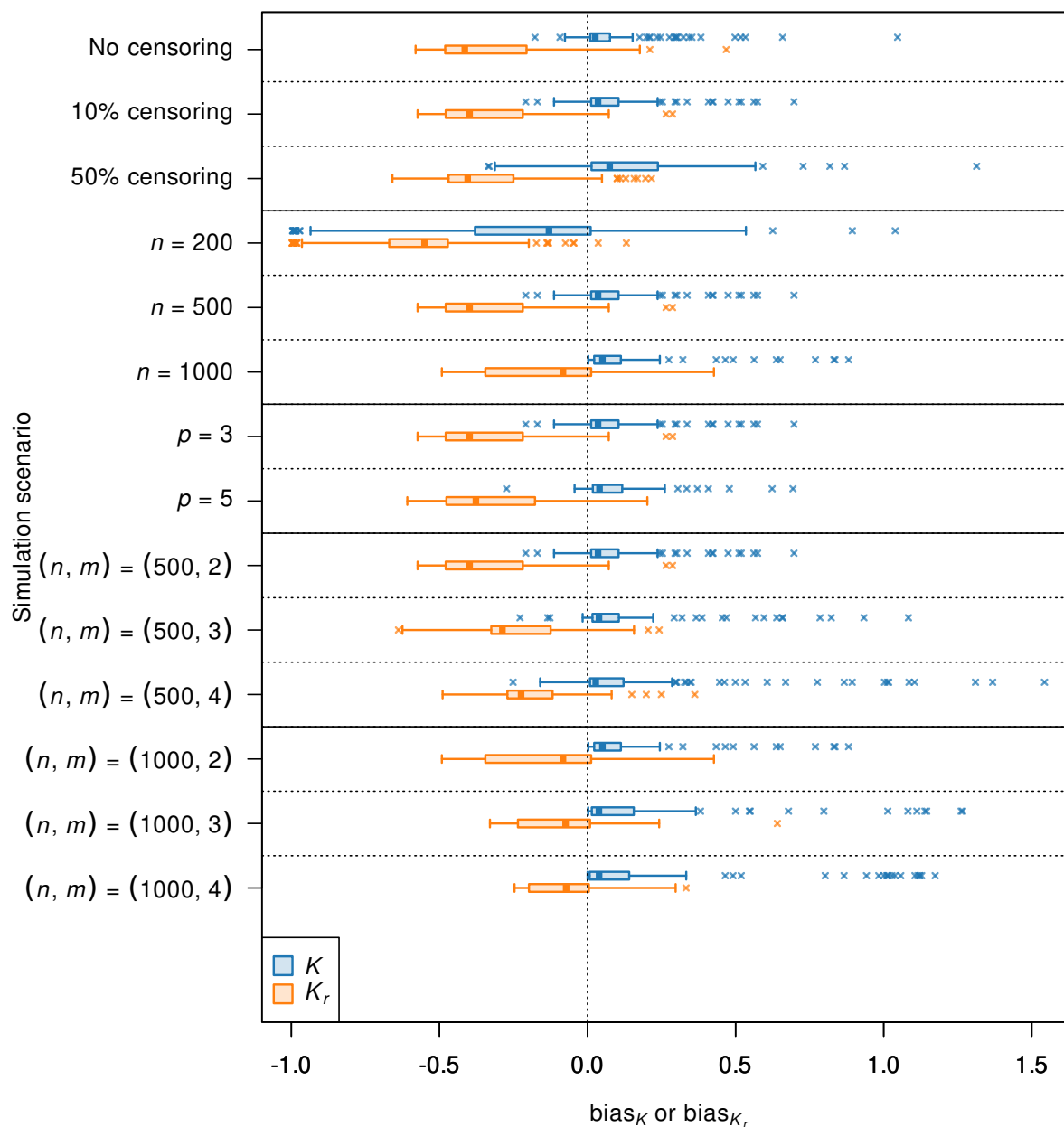
Web Figure 9: Simulation study: For each scenario, we plot the distribution of the average bias of the inference on the regression coefficients  $\beta_{r_j}$  across the 128 replicates from the Multivariate Bernoulli (MVB) detector, maximum likelihood estimation (MLE) and the model by [King and Weiss \(2021\)](#).

and Weiss (2021) perform similarly in terms of  $\text{bias}_\alpha$ . For the regression coefficients, the Multivariate Bernoulli detector overestimates  $\beta_{rj}$  on average for some scenarios where the other two methods perform well, which is likely a result of underestimation of the baseline hazards due to prior shrinkage as shown in Web Figure 8. We note that, nonetheless, the Multivariate Bernoulli detector performs best in terms of mean squared error as shown in Web Figure 7. The results suggest that the shrinkage induced by the prior specification in the Multivariate Bernoulli detector increases bias but reduces variance even more, resulting in lower error compared to the other two methods. This is typical of shrinkage methods such as the James-Stein estimator and Bayesian shrinkage priors in general (e.g. Polson and Sokolov, 2019).

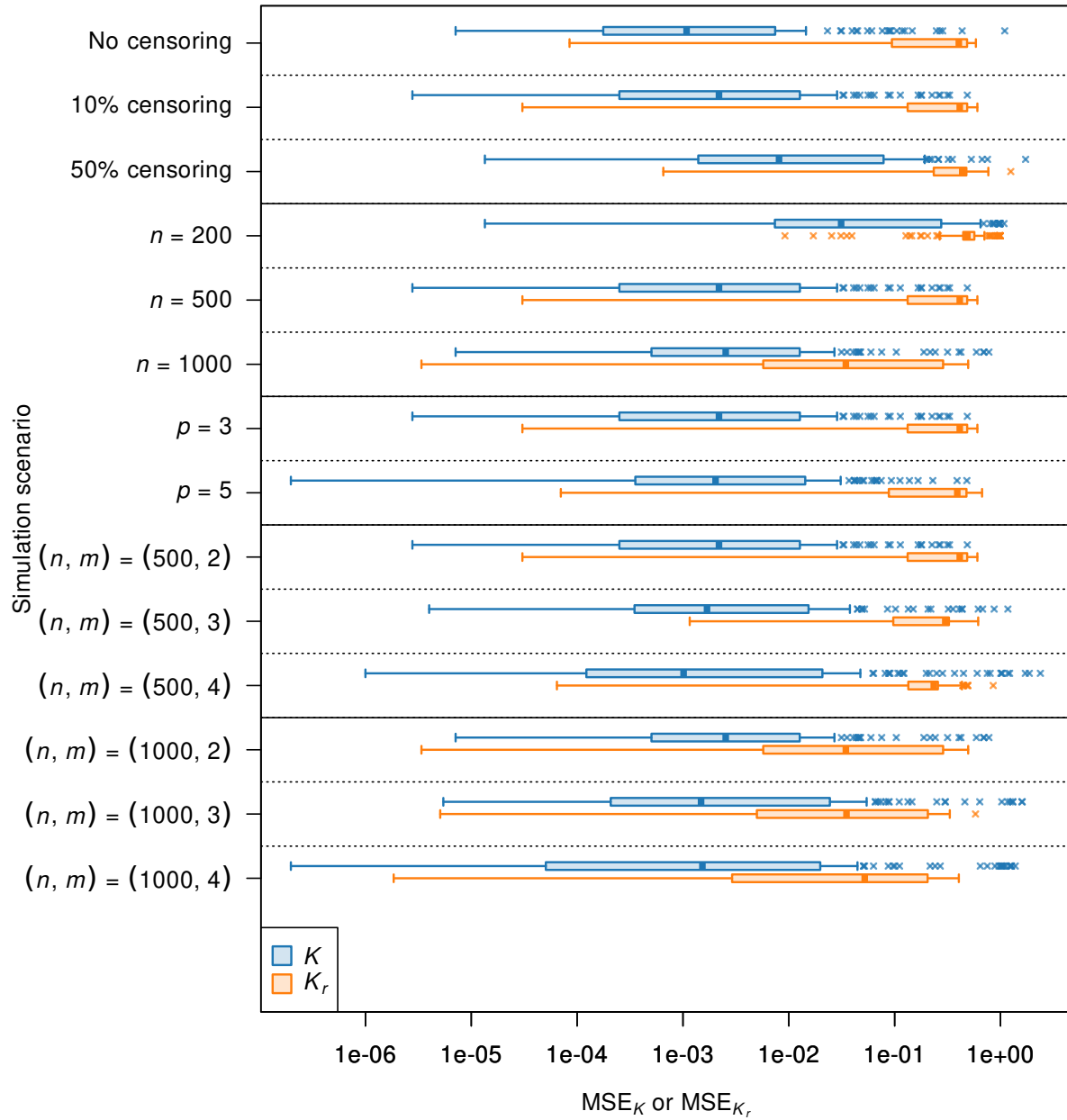
Inference on the number of change points is presented in Web Figure 10. Recall that the MLE and the model by King and Weiss (2021) do not estimate number of change points. The number of cause-specific change points  $K_r$  is typically underestimated while the number of overall change points  $K$  is overestimated by our approach. This is unsurprising since multiple cause-specific change points constitute a single overall change points in the simulation scenarios. Note that data from multiple risks provide information on the number and location of overall change points. On the other hand, a cause-specific change point is inferred from the event rate for a specific risk. This could be a potential explanation for why the mean squared error for  $K$  is typically lower than for  $K_r$  in Web Figure 11.

## E.4 Simulation study on restricting change point locations

Section 2.3.1 of the main manuscript discusses how the prior on the time locations of overall change points  $p(\boldsymbol{\gamma} \mid K) = 1/\binom{|\mathcal{T}|}{K}$  is restricted to a subset of times  $\mathcal{T}$ . Here, we empirically investigate the effect of such constraint. Specifically, we compare with the alternative prior choice  $p(\boldsymbol{\gamma} \mid K) = 1/\binom{t_{\max} - 1}{K}$  which does not have the restriction. Firstly, removing the restriction in the simulation study in Web Section E.3 does not change results notably (results



Web Figure 10: Simulation study: For each scenario, we plot the distribution of the average bias of the inference on the number of change points  $K$  and cause-specific change points  $K_r$  across the 128 replicates from the Multivariate Bernoulli detector.

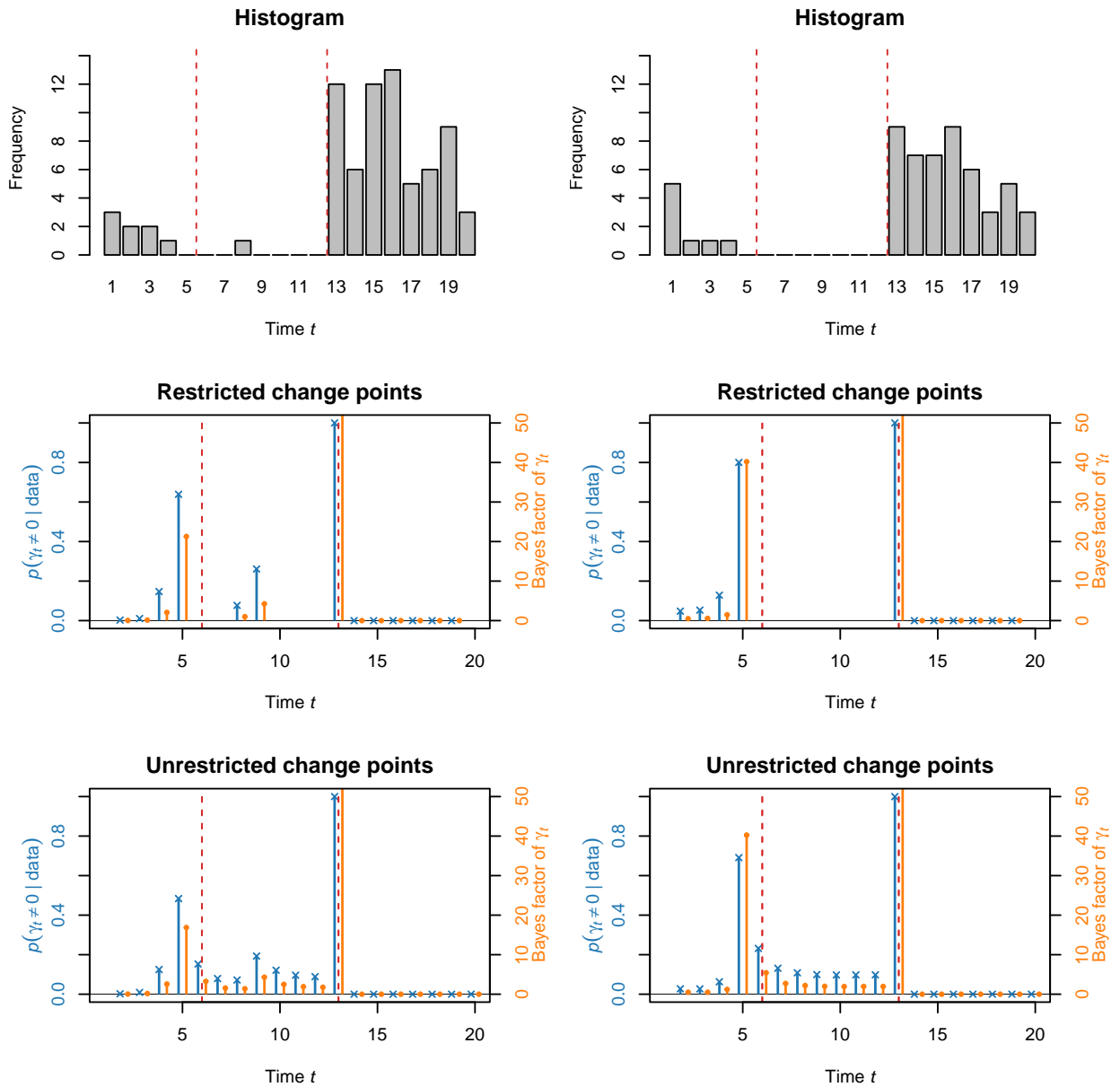


Web Figure 11: Simulation study: For each scenario, we plot the distribution of the mean squared error (MSE) of the inference on the number of change points  $K$  and cause-specific change points  $K_r$  across the 128 replicates from the Multivariate Bernoulli detector.

not shown): there, most simulated data sets have observed events at all time points, such that the restriction does not change the prior  $p(\boldsymbol{\gamma} \mid K)$  notably.

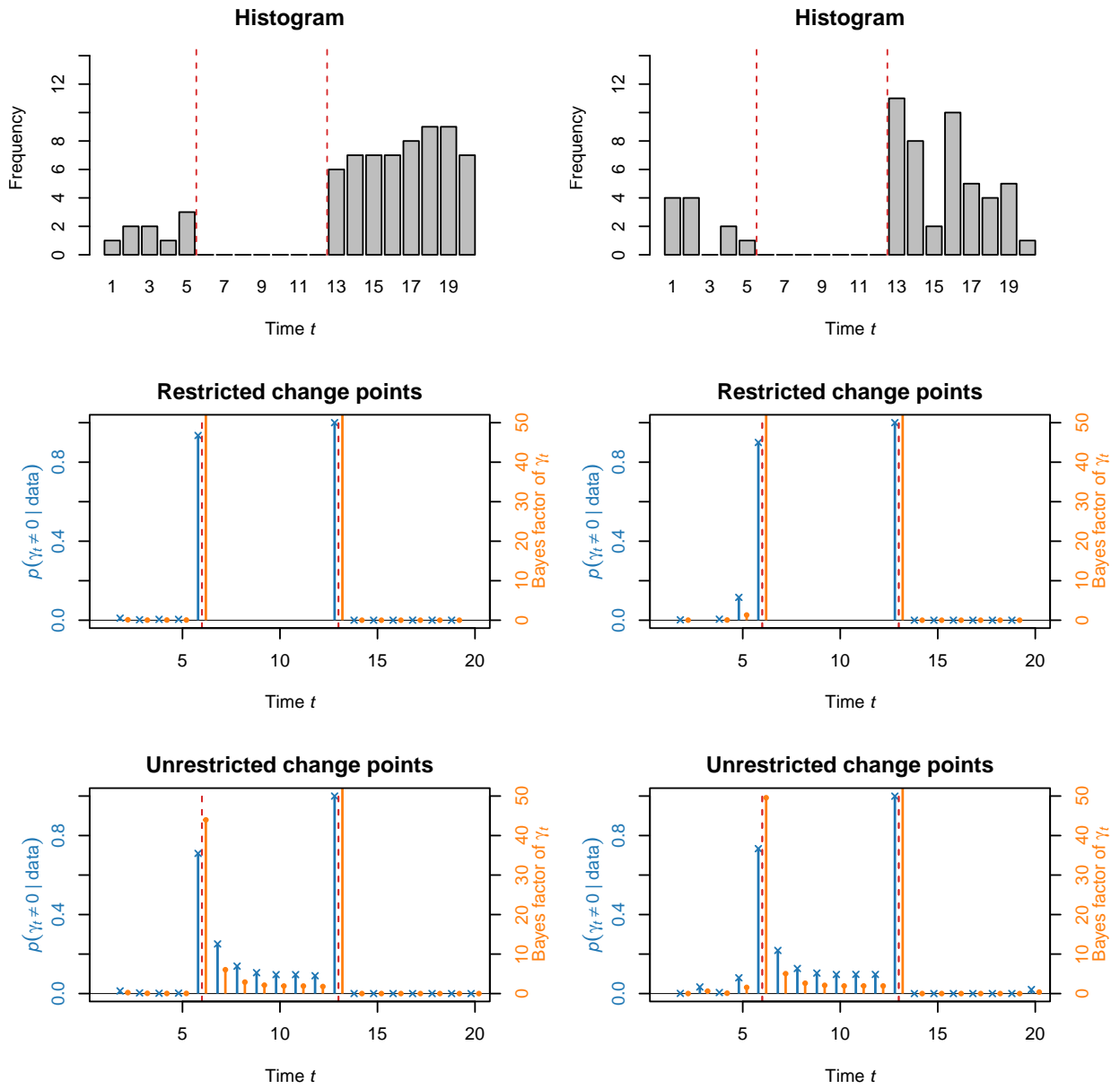
We simulate data with  $n = 100$  observations, no predictors ( $p = 0$ ),  $m = 1$  risk,  $t_{\max} = 15$ , change points at  $t = 6, 13$  and corresponding baseline hazard across change points given by  $(\alpha_{1,1}^*, \alpha_{1,2}^*, \alpha_{1,3}^*) = (-4, -9, -2)$ . We consider four replicated data sets. Two data sets, shown in Web Figure 12, have no observed events near time  $t = 6$  and, thus, a change point at  $t = 6$  is not allowed in the Multivariate Bernoulli detector. The other two, shown in Web Figure 13, have observed events near  $t = 6$ . Then, a change point at  $t = 6$  is allowed in the Multivariate Bernoulli detector.

For each replicate data set, we fit the Multivariate Bernoulli detector as described in Section E.2 as well as the analogous model without a restriction on change point locations, i.e. with  $p(\boldsymbol{\gamma} \mid K) = 1/\binom{t_{\max}-1}{K}$ . The resulting inference on change point locations is summarized in Web Figures 12 and 13. In Web Figure 12, the restriction on change points does not allow inferring the true change point at  $t = 6$ . However, also without the restriction, the posterior probability of a change point at  $t = 5$  is higher than at  $t = 6$ . As such, the restriction does not reduce the quality of inference in the scenario where the true change point  $t = 5$  is not in the support of the restricted prior. On the other hand, omitting the restriction results in posterior mass on spurious change points at times without observed event for all four replicate data sets (see both Web Figures 12 and 13).



Web Figure 12: Simulation study: Histograms of observed event times (top row), and posterior probabilities ( $\times$ ) and Bayes factors ( $\bullet$ ) for the presence of a change point for the model with restricted (middle row) and unrestricted (bottom row) change point locations for the two simulated data sets (left and right columns) with no observed events near time  $t = 6$ . Orange lines correspond to Bayes factors, some of which are outside the plotting range. The dashed red lines are drawn in correspondence of the true change points.





Web Figure 13: Simulation study: Histograms of observed event times (top row), and posterior probabilities ( $\times$ ) and Bayes factors ( $\bullet$ ) for the presence of a change point for the model with restricted (middle row) and unrestricted (bottom row) change point locations for the two simulated data sets (left and right columns) with observed events near time  $t = 6$ . Orange lines correspond to Bayes factors, some of which are outside the plotting range. The dashed red lines are drawn in correspondence of the true change points.

## Web Appendix F Introduction to R package

The R package `mvb.detector`, available from <https://github.com/willemvandenboom/mvb-detector>, implements the Multivariate Bernoulli detector. Here, we provide an introduction on how to use the package.

### F.1 Load and preprocess data

As example data, we consider the data set on unemployment duration from [McCall \(1996\)](#), which is available from the R package `Ecdat`.

```
data("UnempDur", package = "Ecdat")
```

The data provide information on the time new employment after losing a job. That is, the event of interest is finding a new job, and time to event is measured from the loss of the previous job. The times are recorded discretely, in two week intervals. For instance,  $T_i = 6$  means that the time between jobs is twelve weeks. Furthermore, new employment is either full-time or part-time, which represent  $m = 2$  competing risks that can terminate the spell of unemployment.

For simplicity, we consider the subset of cases that are right-censored (i.e. `sensor4 = 1`) or for which it is known whether the new employment is full- or part-time (i.e. `sensor1 = 1` or `sensor2 = 1`).

```
UnempDur_sub <- subset(UnempDur, sensor1 | sensor2 | sensor4)
```

Inspired by the function `dataLongCompRisks` from the R package `discSurv`, `mvb.detector` requires that data are provided as a data frame with the following variables:

1. As first variable, an integer vector `time` with the time-to-event data
2. As second variable, a factor `event` of event types/causes with the first level indicating

that the time was censored

3. Optionally, additional variables that are treated as predictor values

We create such data frame where we include `ui` and standardized `disrate` as covariates:

1. The variable `ui` is a binary indicator of whether the person received benefits from an unemployment insurance scheme.
2. The variable `disrate` is the disregard rate: the *disregard* is the amount that a person is allowed to earn in a new job without reduction in unemployment benefits. The *disregard rate* is the disregard divided by the earnings in the lost job.

Finally, we right-censor all unemployment spells longer than  $t = 10$  to reduce the range of time points for ease of exposition.

```
UnempDur_sub$event <- 0L
UnempDur_sub$event [UnempDur_sub$censor1 == 1] <- 1L
UnempDur_sub$event [UnempDur_sub$censor2 == 1] <- 2L

# Right-censor unemployment spells longer than 10.
UnempDur_sub$event [UnempDur_sub$spell > 10] <- 0L
UnempDur_sub$spell <- pmin(10, UnempDur_sub$spell)

UnempDur_sub$event <- factor(x = UnempDur_sub$event, levels = 0:2)
levels(UnempDur_sub$event) <- c("censored", "Full-time", "Part-time")

data <- data.frame(
  time = as.integer(UnempDur_sub$spell), event = UnempDur_sub$event,
  X = cbind(UnempDur_sub$ui == "yes", scale(UnempDur_sub$disrate))
)
```

```
summary(data)
```

```
##           time           event           X.1           X.2
## Min.      : 1.000   censored :1449   Min.      :0.0000   Min.      : -1.4689
## 1st Qu.:  2.000   Full-time: 919   1st Qu.:0.0000   1st Qu.: -0.7870
## Median :  5.000   Part-time: 299   Median :1.0000   Median : -0.1050
## Mean    :  5.311                               Mean    :0.5778   Mean     :  0.0000
## 3rd Qu.:  9.000                               3rd Qu.:1.0000   3rd Qu.:  0.5352
## Max.    :10.000                               Max.    :1.0000   Max.    :12.6986
```

## F.2 Fit the Multivariate Bernoulli detector

We fit the Multivariate Bernoulli detector to the data using 20000 Markov chain Monte Carlo (MCMC) iterations, discarding the first 10000 as burn-in.

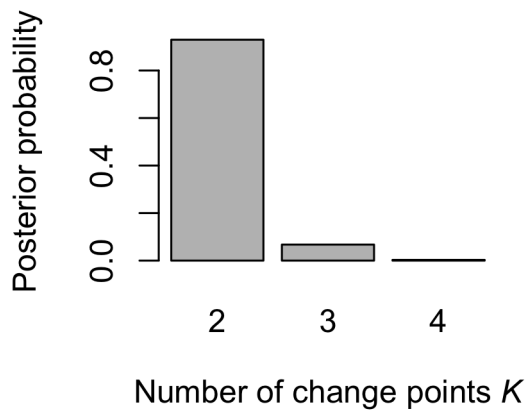
```
set.seed(1L) # Set seed for reproducibility.

mvbd_fit <- mvb.detector::run_mvbd_detector(
  data = data, n_iter = 2e4L, burnin = 1e4L
)
```

## F.3 Summarize posterior inference

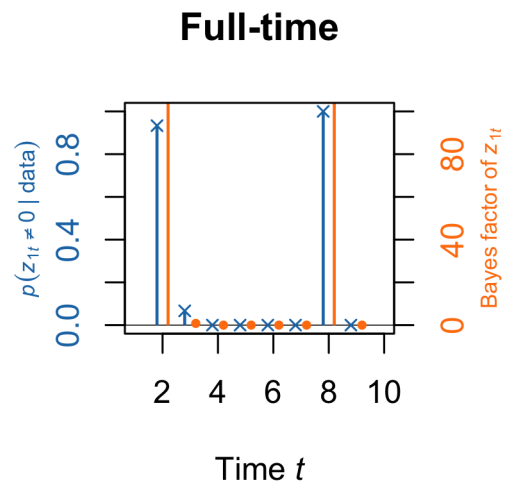
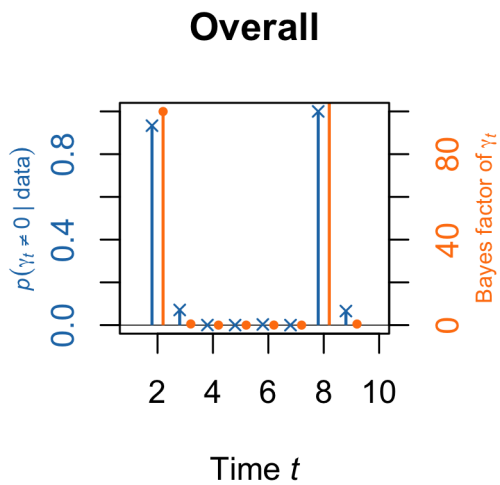
The MCMC iterations are now saved in `mvbd_fit`. The package provides a variety of functions to summarize the corresponding posterior inference. Firstly, we plot the posterior on the number of change points, and find that the posterior concentrates on two change points.

```
mvb.detector::plot_K(mvbd_fit)
```

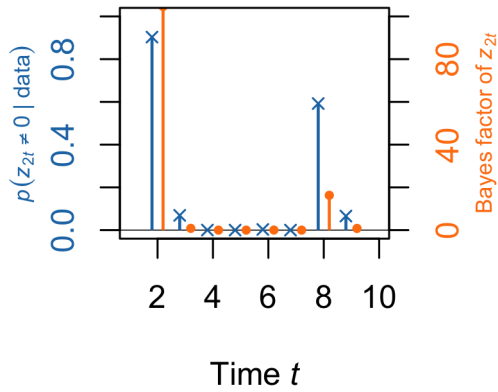


To inspect the location of the change points, we plot posterior inclusion probabilities and Bayes factors:

```
par(mar = c(5, 4, 4, 4)) # Increase right margin to make space for labels.
mvb.detector::plot_change_points(mvbd_fit)
```

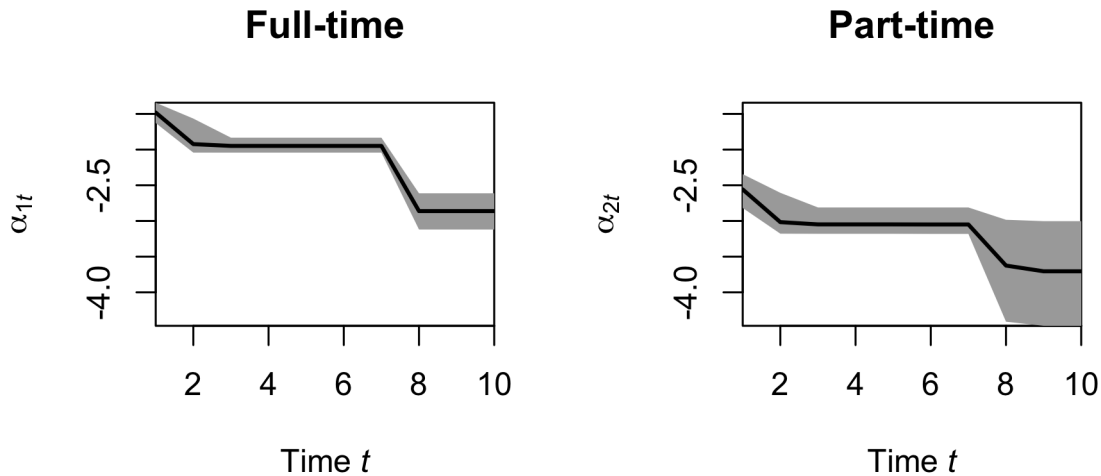


## Part-time



The change points are mostly at  $t = 2$  and  $t = 8$  in the posterior distribution. The second change point ( $t = 8$ ) might not be present for the hazard rate specific to part-time re-employment. The posterior mean and 95% credible intervals of the baseline hazards are consistent with this:

```
mvb.detector::plot_baseline_hazards(mvbd_fit)
```



For the regression coefficients, we can compute posterior inclusion probabilities, and plot posterior means and 95% credible intervals. In the output below, no effect of disregard rate

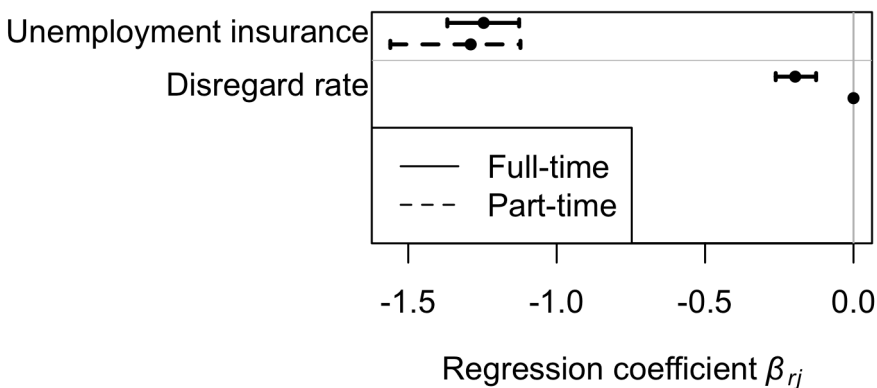
on part-time re-employment is inferred. At the same time, the other covariate effects are negative: employment benefits are associated with a longer time to re-employment. The same holds for disregard rate and full-time re-employment. A potential explanation is that those with a higher disregard rate prefer to take a part-time job instead of a full-time job to maximize unemployment benefits, which is in line with Table III of [McCall \(1996\)](#).

```
pred_names <- c("Unemployment insurance", "Disregard rate")

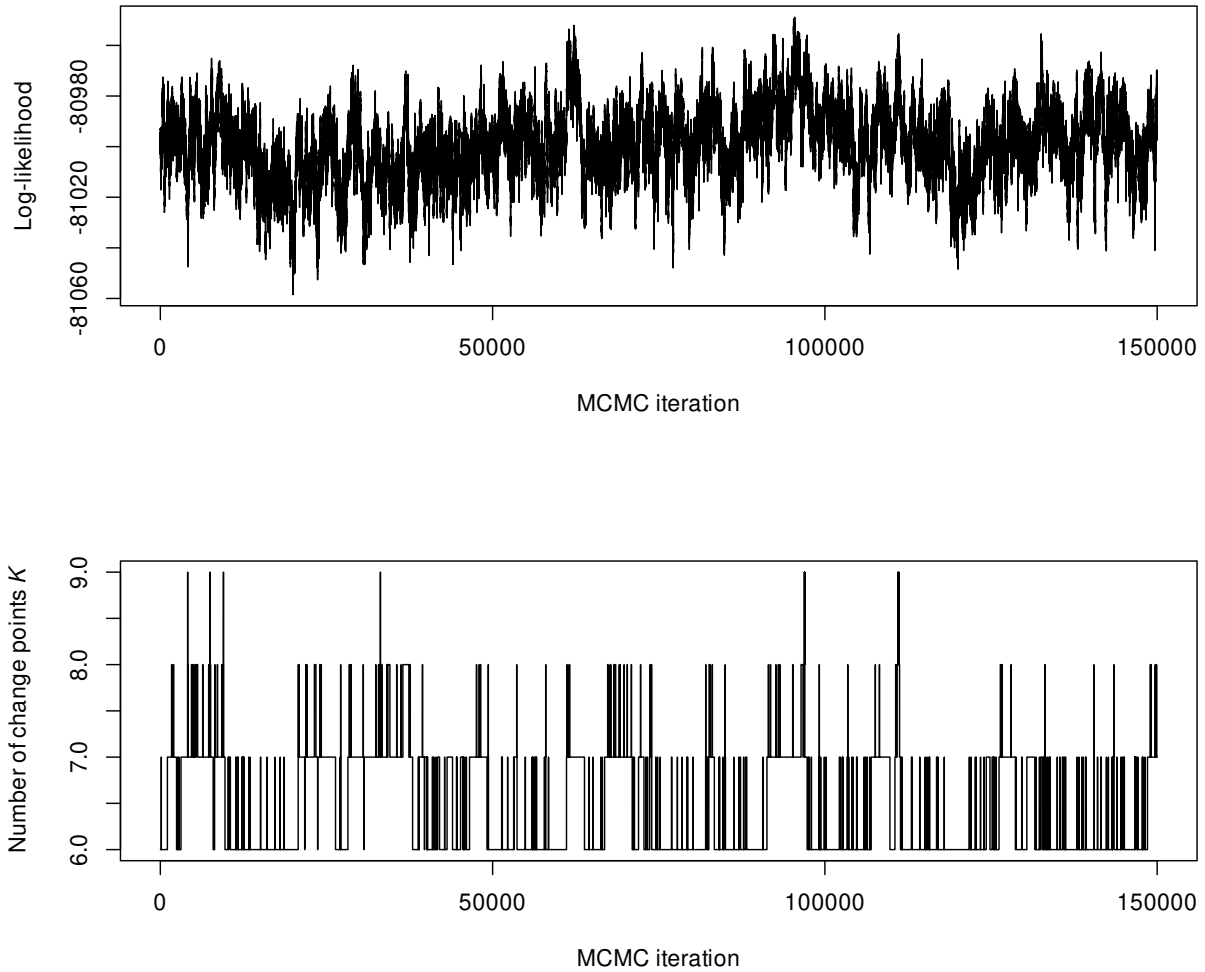
mvd.detector::compute_post_inc_prob(
  mvbd_fit = mvbd_fit, pred_names = pred_names, digits = 3L
)
```

```
##                Full-time Part-time
## Unemployment insurance      1      1.000
## Disregard rate              1      0.001
```

```
par(mar = c(5, 10, 4, 2)) # Increase left margin to makes space for labels.
mvd.detector::plot_regression(mvbd_fit = mvbd_fit, pred_names = pred_names)
```

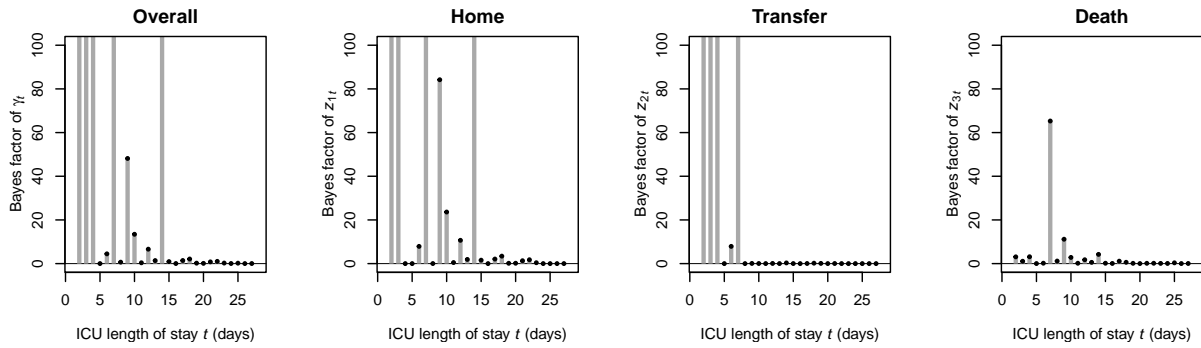


## Web Appendix G Additional figures

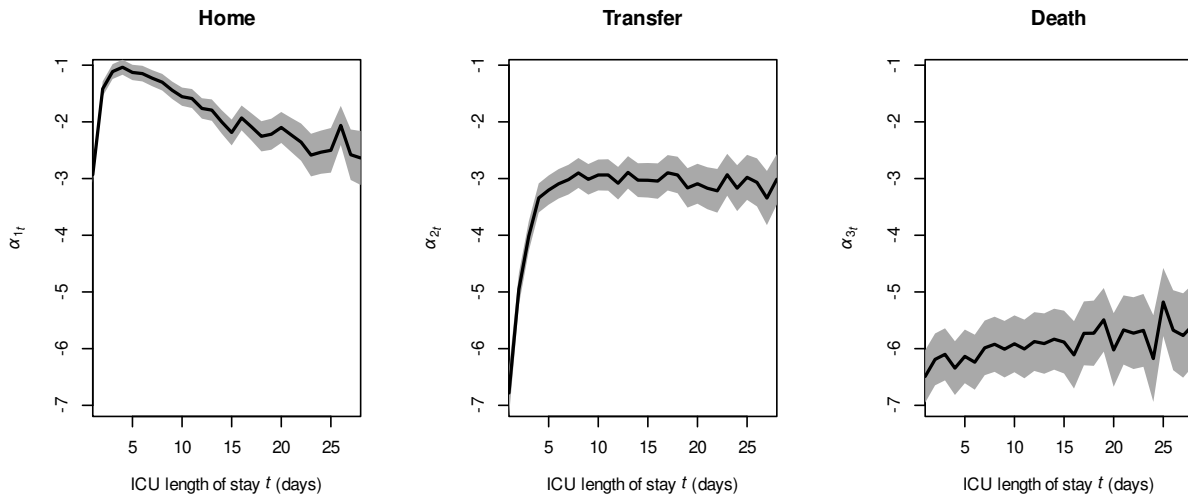


Web Figure 14: ICU data: Trace plots of the MCMC chain for the log-likelihood  $\log\{p(\text{data} \mid \boldsymbol{\theta})\}$  and number of change points  $K$ .

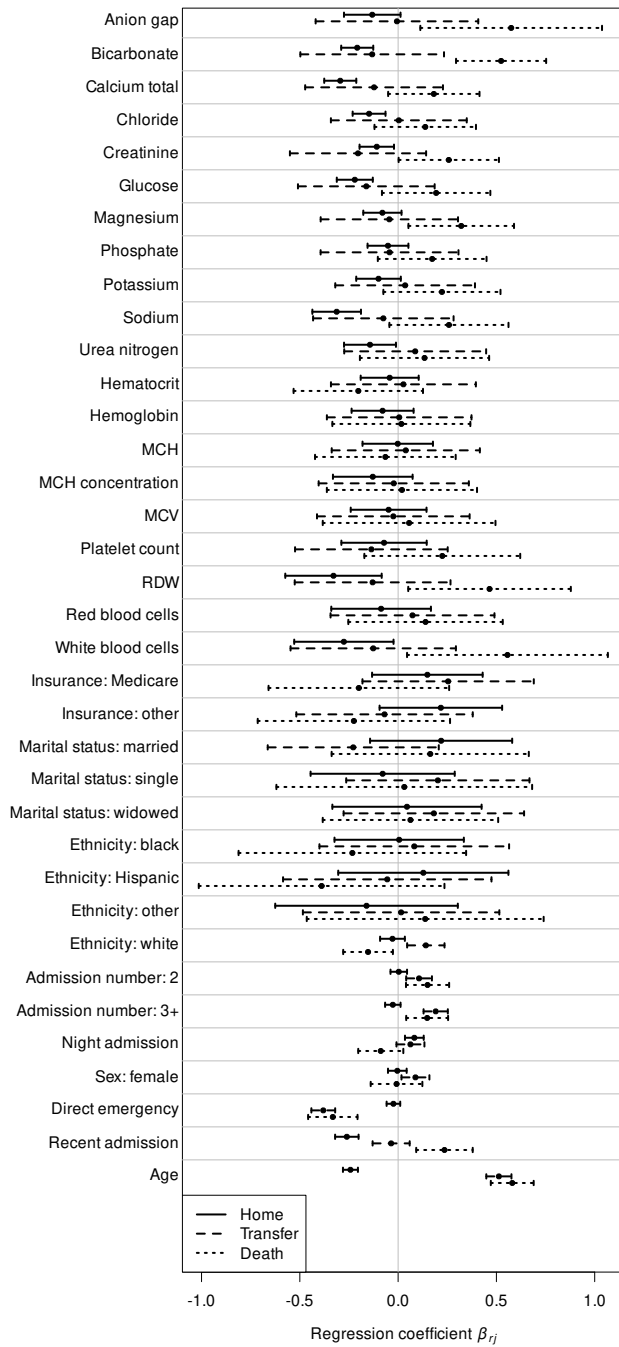




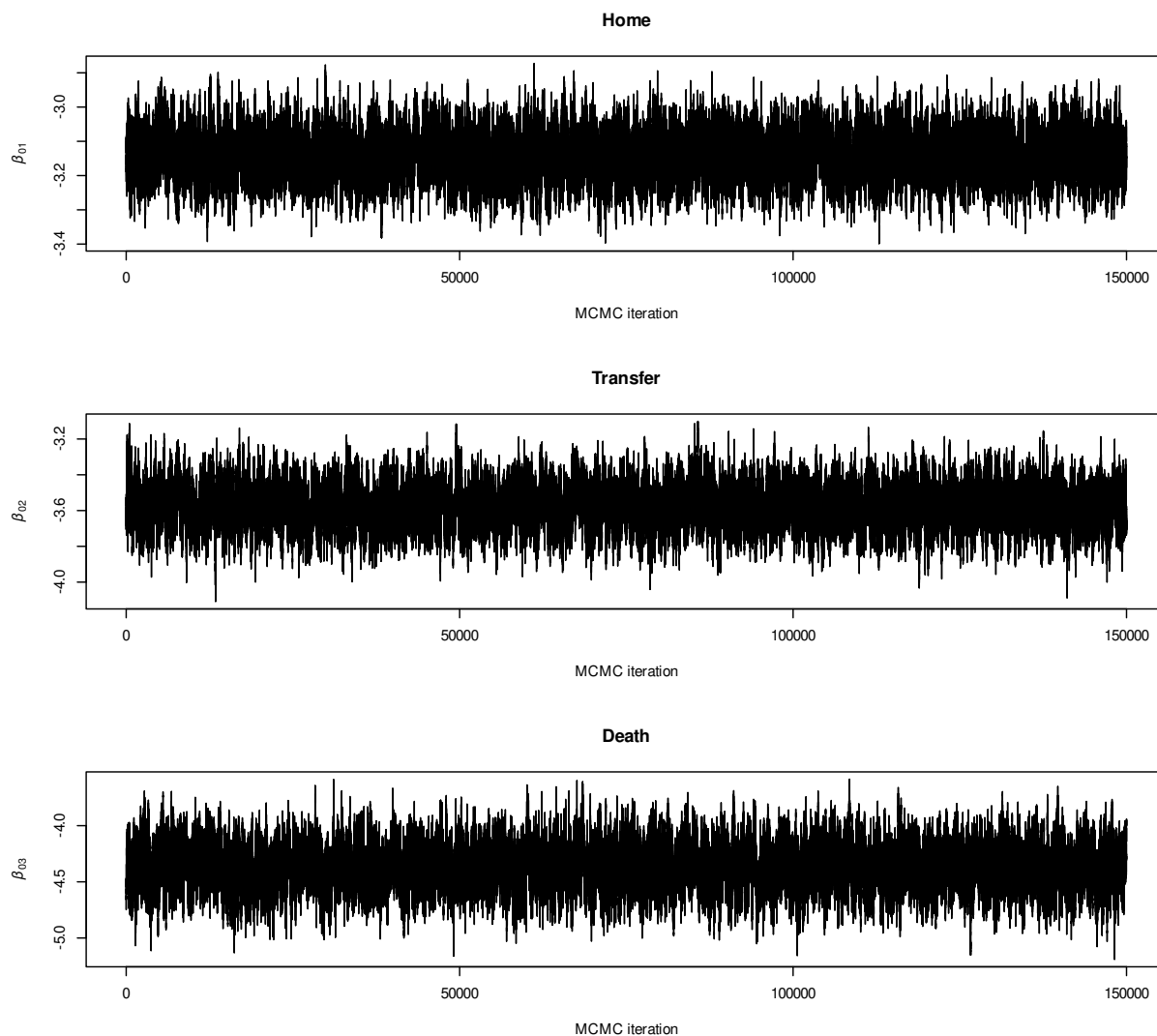
Web Figure 15: ICU data: Bayes factors for the presence of a change point for the overall (left column) and cause-specific (other columns) hazard functions. The gray lines correspond to Bayes factors, some of which are outside the plotting range.



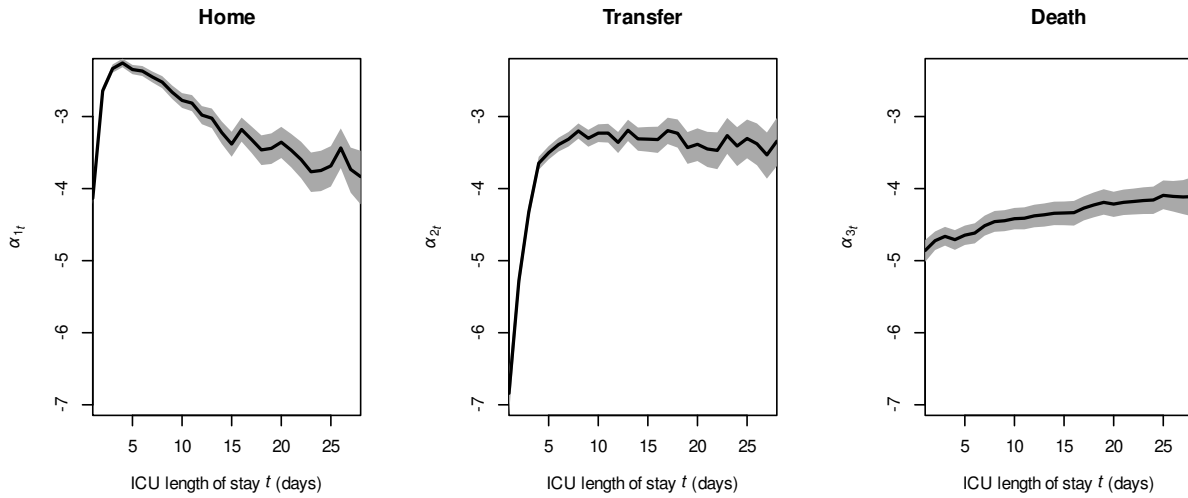
Web Figure 16: ICU data: Maximum likelihood estimates of the baseline hazard parameter  $\alpha_{rt}$  (lines) with their 95% confidence intervals demarcated by shaded areas.



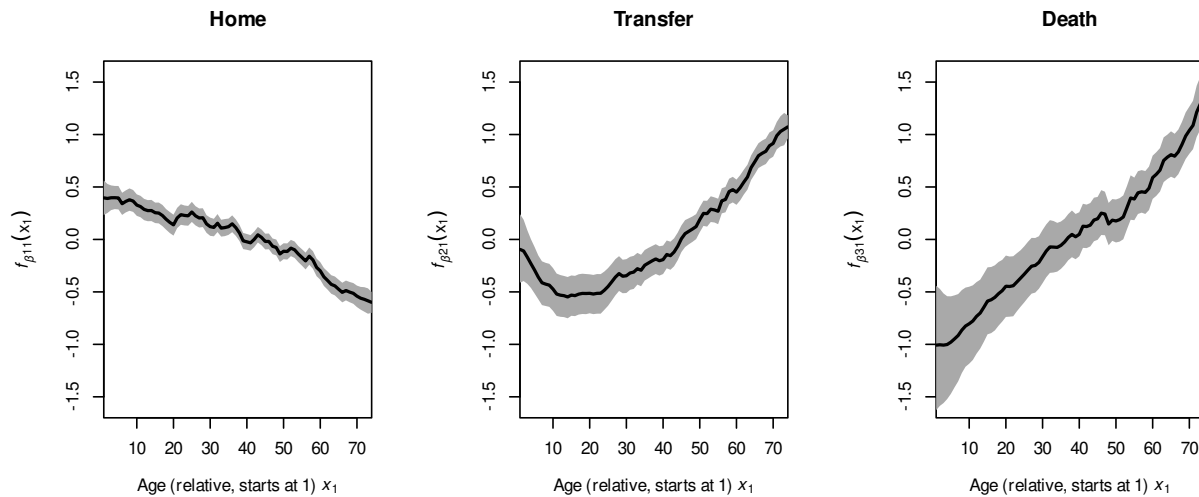
Web Figure 17: ICU data: Maximum likelihood estimates (dot) and 95% confidence intervals (lines) of the regression coefficients for each risk. The categorical predictors are coded as dummy variables as detailed in Web Appendix A. MCH stands for mean cell hemoglobin, MCV for mean corpuscular volume and RDW for red blood cell distribution width.



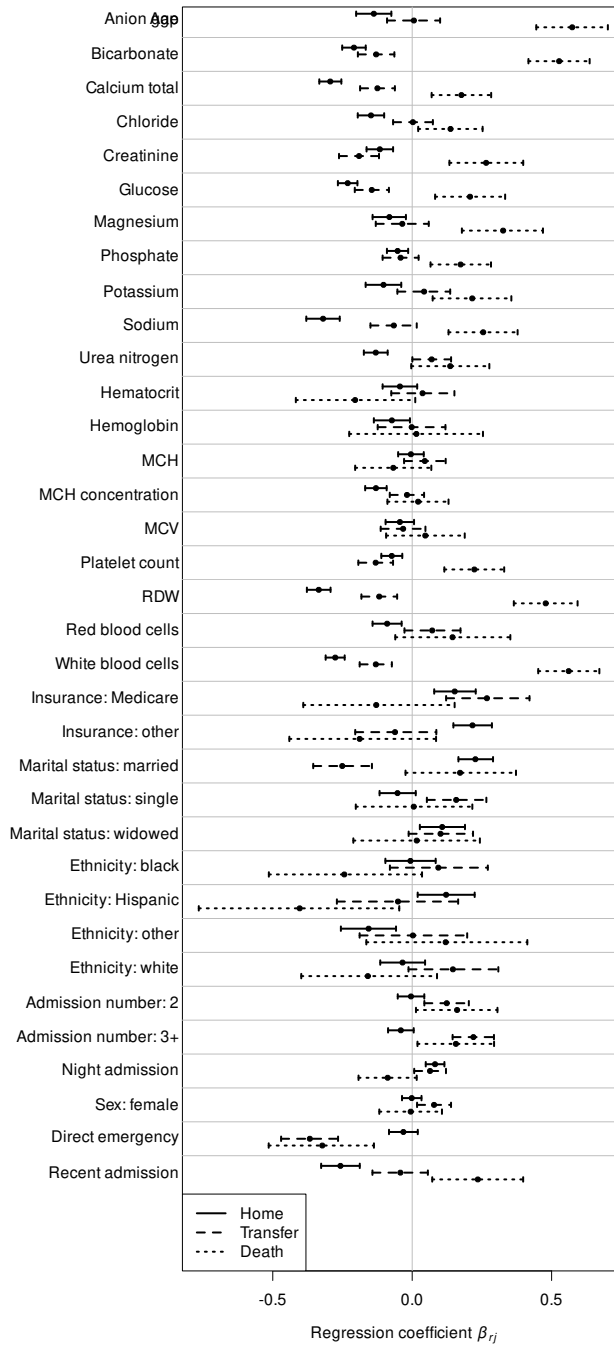
Web Figure 18: ICU data: Trace plots of the MCMC chain for the intercepts  $\beta_{0r}$  in the model by [King and Weiss \(2021\)](#). Trace plots for other parameters show similarly good mixing (not shown).



Web Figure 19: ICU data: Posterior inference on the baseline hazard parameter  $\alpha_{rt}$  from the model by [King and Weiss \(2021\)](#). Lines represent posterior means and shaded areas correspond to 95% credible intervals.



Web Figure 20: ICU data: Posterior inference on  $f_{\beta_{r1}}(x_1)$ , where  $x_1$  denotes *age*, obtained with the model by [King and Weiss \(2021\)](#). Lines represent posterior means and shaded areas correspond to 95% credible intervals. Here, age is in years on a relative scale with  $x_1 = 1$  corresponding to the youngest patient and  $x_1 = 74$  with the oldest.



Web Figure 21: ICU data: Maximum likelihood estimates (dot) and 95% confidence intervals (lines) of the regression coefficients for the binary predictors from the model by King and Weiss (2021) for each risk. The categorical covariates are coded as dummy variables as detailed in Web Appendix A. MCH stands for mean cell hemoglobin, MCV for mean corpuscular volume and RDW for red blood cell distribution width.

## References

- Creswell, R., Lambert, B., Lei, C. L., Robinson, M., and Gavaghan, D. (2020). Using flexible noise models to avoid noise model misspecification in inference of differential equation time series models. arXiv:2011.04854v1.
- Dahl, D. B. (2005). Sequentially-allocated merge-split sampler for conjugate and nonconjugate Dirichlet process mixture models. Technical report, Department of Statistics, Texas A&M University.
- Dickey, J. M. (1971). The weighted likelihood ratio, linear hypotheses on normal location parameters. *The Annals of Mathematical Statistics* **42**, 204–223.
- Frühwirth-Schnatter, S. and Frühwirth, R. (2007). Auxiliary mixture sampling with applications to logistic models. *Computational Statistics & Data Analysis* **51**, 3509–3528.
- Goldberger, A. L., Amaral, L. A. N., Glass, L., Hausdorff, J. M., Ivanov, P. C., Mark, R. G., Mietus, J. E., Moody, G. B., Peng, C.-K., and Stanley, H. E. (2000). PhysioBank, PhysioToolkit, and PhysioNet. *Circulation* **101**, e215–e220.
- Held, L. and Holmes, C. C. (2006). Bayesian auxiliary variable models for binary and multinomial regression. *Bayesian Analysis* **1**, 145–168.
- Johnson, A., Bulgarelli, L., Pollard, T., Horng, S., Celi, L. A., and Mark, R. (2022). MIMIC-IV (version 2.0). *PhysioNet*. <https://doi.org/10.13026/7vcr-e114>.
- Johnson, A. E. W., Bulgarelli, L., Shen, L., Gayles, A., Shammout, A., Horng, S., et al. (2023). MIMIC-IV, a freely accessible electronic health record dataset. *Scientific Data* **10**, 1.
- King, A. J. and Weiss, R. E. (2021). A general semiparametric Bayesian discrete-time recurrent events model. *Biostatistics* **22**, 266–282.

- Legramanti, S., Rigon, T., and Durante, D. (2022). Bayesian testing for exogenous partition structures in stochastic block models. *Sankhya A* **84**, 108–126.
- Martínez, A. F. and Mena, R. H. (2014). On a nonparametric change point detection model in Markovian regimes. *Bayesian Analysis* **9**, 823–858.
- McCall, B. P. (1996). Unemployment insurance rules, joblessness, and part-time work. *Econometrica* **64**, 647–682.
- Meir, T. and Gorfine, M. (2023). Discrete-time competing-risks regression with or without penalization. arXiv:2303.01186v2.
- Polson, N. G. and Sokolov, V. (2019). Bayesian regularization: From Tikhonov to horseshoe. *WIREs Computational Statistics* **11**, e1463.
- Verdinelli, I. and Wasserman, L. (1995). Computing Bayes factors using a generalization of the Savage-Dickey density ratio. *Journal of the American Statistical Association* **90**, 614–618.